THE INFLUENCE OF STRESS MAGNITUDE AND STRESS HISTORY
ON DAMPING, PLASTICITY, AND FATIGUE PROPERTIES
OF METALLIC MATERIALS

L. J. DEMER
and
B. J. LAZAN

DEPARTMENT OF MECHANICS AND MATERIALS

UNIVERSITY OF MINNESOTA

Minneapolis, Minnesota
September 1958

BEST AVAILABLE COPY

THE EFFECT OF STRESS MAGNITUDE AND STRESS HISTORY ON THE DAMPING, ELASTICITY, AND FATIGUE PROPERTIES OF METALLIC MATERIALS

L. J. DEMER
and
B. J. LAZAN

Minneapolis, Minnesota
September 1953

FOREWORD

ABSTRACT

A general treatment of the damping field is presented dealing with factors involved in the experimental determination of the damping properties of materials, particularly at engineering stress levels. The relationships among damping, elasticity, and fatigue are discussed. The research program at the University of Minnesota in this field is described, and the results of past work are reviewed. Data obtained from rotating cantilever beam tests at room temperature are presented on the damping, elasticity, and fatigue properties of a variety of metallic materials over a wide range of stresses. The damping and elasticity data were obtained at a frequency of 20 rpm. The existence of a damping cyclic stress sensitivity limit for all materials tested is shown. Various stress history effects above the cyclic stress sensitivity limits are indicated. Slopes for the logarithmic plot of damping vs. stress are investigated throughout the range of test stresses employed. Dynamic stress-strain curves are presented and the variation of dynamic modulus of elasticity as a function of stress for the various materials is indicated. Comparisons are made among the damping and elasticity properties of the materials. An approximate relationship between damping and the fatigue and tensile strengths is shown. Problems to be studied in future investigations are mentioned. An Appendix is included in which equations are developed for interpreting rotating cantilever beam data so that the effective length of specimen fillets, and specific damping energy and dynamic secant modulus of elasticity may be calculated.

TABLE OF CONTENTS

LIST OF TABLES

LIST OF FIGURES

I. INTRODUCTION

The properties of materials under sustained cyclic stress of both constant and variable magnitude have received considerable attention in the past, yet the situation remains uncomfortably confused. Also, there is inconsistency in the literature regarding the effects of testing variables, notably stress magnitude and stress history, on the damping properties of materials, and the general interpretation of damping and its significance in engineering design. To aid in clarifying these factors and correlating the general behavior of materials under cyclic stress (as defined by their 'dynamic' properties), a broad program of study is currently in progress at the University of Minnesota. One phase of this program is concerned with the evaluation of, and correlation among damping capacity, dynamic modulus of elasticity, fatigue, and dynamic stress-strain characteristics of materials under sustained cyclic stress of both constant and gradually increasing magnitude. The broad program also includes a detailed study of the variables which affect damping energy.

The specific objectives of the work covered in this paper will be discussed after prior work has been reviewed.

II. REVIEW OF PRIOR WORK

2.1 General

For several decades various investigators have been concerned with the damping property of materials, or their ability to dissipate vibrational energy. From these studies many conflicting and often directly contradictory statements have resulted, not only in regard to the factors affecting damping, but also in comparisons of the relative damping properties of various materials. No attempt will be made here to present a complete survey of the voluminous mass of literature available in this field, for several summaries of the principal results of prior investigations have been published in recent years. Among these are the publications of Kimball (1), Hatfield, Stanfield, and Rotherham (2), Thompson (3), Potter (4), and Linacre (5). A discussion will be given, however, of various factors involved in the experimental determination of damping particularly at the higher stress levels.

2.2 Expressions for Damping

A complicating factor in reviewing prior work is in the different methods employed for expressing the dissipation of vibrational energy. Potter (4) presents an able discussion of this problem and explains that at least eight units have been proposed and used for stating this property quantitatively. Some of these are expressions of the energy losses themselves, whereas others give the relation between the energy losses and the elastic energy involved.

Two materials with equal energy losses in absolute value will behave differently if their elastic energies differ. For example, the rate of vibration decay in a material depends not only on the damping energy, but also on its modulus of elasticity. Here the ratio of the energies involved in damping and elasticity is the important factor rather than their absolute values. On the other hand is the practical consideration that a given machine component may be required to dissipate a given amount of vibrational energy input resulting from some characteristic of the application and yet contribute little elasticity to the system. If the part is able to do this for vibrational stress amplitudes within the allowable fatigue strength of the

1

material, then the material is satisfactory for the application. In this case, consideration of the absolute energy dissipated is important. Furthermore, in the analysis of the resonance response of members it is also desirable, if not essential, to consider the absolute energy dissipation of the parts. Methods for dealing with this problem are outlined in recent papers by Cochardt (6) and Lazan (7).

In summary, for a determination of the effect of different variables upon the damping ability of a given material, either of the two methods of expressing damping discussed above is satisfactory. When different materials are to be compared, however, for applications involving stresses remote from possible fatigue failure, then expressions which involve the ratio of damping to elastic energy are suitable because the relative moduli of elasticity are thus considered. For applications in which energy dissipation within the material is important in order to keep resonant stresses and amplitudes within safe values, then expressions for damping in terms of absolute energy are desirable. At the same time, however, consideration must be given to the relative elastic moduli and also to the fatigue strengths of the different materials.

Expressions which have been used most widely for relating the damping and elastic energies are the terms "logarithmic decrement" and "specific damping capacity." The "logarithmic decrement" is the natural logarithm of the ratio of the maximum amplitude of two successive cycles of a freely vibrating body. The term "specific damping capacity" is defined as the ratio of the energy loss per cycle to the potential energy of maximum stress.

For an expression of absolute energy, Föppl (8) defines "damping capacity" as the amount of work dissipated into heat in a unit volume of material during a completely reversed cycle of unit stress. "Internal friction" as used by Zener (9) refers to the capacity of a solid to convert its mechanical energy of vibration into internal energy. There are objections to both of these definitions because, as Thompson (3) points out, they partially commit themselves to explanations of the phenomenon which is not at present well understood.

A term which may be used to express absolute energy without such interpretive definition is merely "damping energy" which refers to the energy dissipated per cycle of reversed stress. In recent papers by Lazan and his co-workers this has been employed with various restrictive adjectives. "Total damping energy" is used to refer to the total energy absorbed by the specimen per cycle. The term "average damping energy" is defined by them as the energy absorbed per unit volume of stressed material per cycle. This, like the total damping energy, is not a basic unit since it depends on the type of specimen as well as the stress distribution employed in the tests. Finally, the basic "specific damping energy" is the vibrational energy dissipated per cycle per cubic inch of material under conditions of uniform stress.

2.3 Low and High Stress Damping

Misunderstandings and confusion in regard to the importance of different test variables arose from the findings of many of the earlier investigators in the damping field. This was the result in some cases of the failure to distinguish between differences in the modes of energy dissipation at low stresses, up to a few hundred psi, and that at stress levels of engineering importance. Low stress damping is caused chiefly by microscopic and macroscopic thermoelastic effects, by diffusion, and in certain materials by magnetic effects. At high stresses, although these above mentioned effects still contribute to the total, the major portion of the energy dissipated is the result of plastic deformation. A lucid discussion of these various causes of energy dissipation is presented in a series of articles by Darling (10).

2.4 Variables Affecting Damping

The results of many of the earlier investigators also contain conflicting indications regarding the relative damping properties of various materials. In some cases, this resulted from failure to compare the properties using the same quantitative basis of measurement. For example, comparison of the logarithmic decrement of materials of widely different moduli of elasticity will give a different relative order for a set of materials than when they are compared on the basis of specific damping energy for a given stress. The major source of disagreement, however, in the comparative rating of the damping properties of materials, probably arose from failure to control properly one or more of the significant variables in the experimental work. Under certain conditions, at least, past work has shown that the following factors may significantly affect the damping properties of a material: frequency, stress amplitude, previous stress history (number of cycles at a given stress), temperature, and surrounding magnetic fields. In much of the previous experimental work performed in the higher range of stress, one or more of these factors were ignored in attempts to determine the significance of another variable. Since the effect of these factors on the damping property varies with the material, it is clear that omission of their control in testing widely different materials could produce very conflicting results in the relative properties of the materials. Following is a discussion of several of the important test variables.

2.5 Effect of Frequency

A study of the literature on damping indicates that the stress level of measurement is an important consideration in a determination of the effect of frequency. Discussions of the frequency effect are to be found in the reviews by Kimball (1) and Thompson (3), among others. The experimental results of various investigators summarized by Kimball show beyond question that frequency does have an important effect on the magnitude of damping in the region of very low stresses. Zener (11) has presented a theory for this frequency effect which checks closely the experimental results of Bennewitz and Rotner (12). His theory indicates a maximum in damping to be expected at a definite intermediate frequency depending on the thermoelastic or other properties of the material.

In the region of higher stresses where energy dissipation by plastic action becomes the major factor in damping, the effect of frequency is different than at the low stresses. The work of Hopkinson and Williams (13) initially suggested that there might be about a 30 per cent decrease in the hysteresis at speeds approximately 120 cycles per second as compared with that under static conditions. However, the results of Rowett (14) on thin-walled tubes in torsion demonstrated that the energy dissipated is practically the same at high and low speeds. He reevaluated the data of Hopkinson and Williams, and by using more precise methods of calculation he showed that their static and dynamic results agreed closely.

Several other investigators have since examined the effect of frequency in the higher stress range. The results of some of these will be mentioned. Kimball and Lovell (15) in their experimental study of eighteen different materials (metals, glass, celluloid, rubber, and wood) found the logarithmic decrement to be entirely independent of frequency of stress or strain velocity for frequencies between two or three per minute up to fifty per second, the entire range investigated. According to Foppl (6), there is no frequency effect except at very low frequencies for materials subject to creep, when the frequency is so low that the strain velocity and creep velocity are of the same order of magnitude. Gemant and Jackson (16) studied the internal damping of several solid dielectric materials, Ebonite, Trolitul, quartz, glass, and wood, over a frequency range of 0.3 to 10 cycles per second, and found no effect. Gemant (17) noted no significant variation in the damping of a steel tube at frequencies between 300 and 3600 cycles per second. Contractor and Thompson (18) in work on a variety of steels found no effect on damping over the frequency range of 450 to 790 cycles per minute.

3

The experiments of Robertson and Yorgiadis (19) on Lucite, Bakelite, plywood, magnesium alloys, a nickel alloy, a carbon steel, and an alloy steel, indicated that the damping capacity of materials is independent of frequency of stressing. Their tests covered the range from 10 to 70 cycles per second. It should be noted that in most of the studies described above, the frequency range investigated was not large.

A few experimenters observed a frequency effect in the high stress range, but this may have been caused by failure to prevent variation in stress amplitude or temperature at the different frequencies. Since both of these factors have a major influence on high stress damping, the effect observed may have been the result of two or three factors instead of frequency alone. In a similar fashion, however, the failure of some of the previously mentioned investigators to observe a real frequency effect may also have resulted from a temperature variation during the tests.

2.6 Effect of Stress Amplitude

In reviewing the results of prior investigations, Thompson (3) shows a particularly patternless behavior among various materials for the relationship between damping capacity and stress magnitude. This may be due principally to the failure of some experimenters to control one or more significant test variables, for certain of the studies have shown a much clearer picture of the effect of stress magnitude. Hopkinson and Williams (13) were among the first to demonstrate the stress dependency. They found the energy loss per cycle to vary approximately as the fourth power of the stress amplitude in direct stress tests on a crankshaft steel. Rowett (14) in torsion tests on an annealed hard-drawn steel in the form of thin-walled tubes showed the variation to be approximately as the third power of stress. Kimball and Lovell (15) in rotating beam tests on various materials indicated an approximate variation as the second power of stress for the eighteen materials tested, but they noted that as the elastic limit is approached, the damping begins to rise at a much more rapid rate. The many papers of Ludwik and Lehr on this subject are reviewed by Vitovec and Lazan (20). Their data show that the curve of damping energy plotted as a function of stress, for both low and high damping materials, exhibits an initial portion of relatively constant or slowly increasing damping followed by a rapid rise beyond a given stress value. Spaeth (21), in a summary of previous work, indicates that this general behavior is followed by both ferrous and non-ferrous materials.

For much of the work reported on the effect of stress magnitude, linear scales were used to graph the results. With the damping plotted as energy loss per cycle, the results generally satisfy squared or cubic curves as indicated above. In many cases, however, the damping is expressed in terms of logarithmic decrement or as ψ, the ratio of the damping energy to the maximum elastic energy. In such cases, a variation of damping energy loss with the square of stress gives a constant logarithmic decrement of vibration because the elastic energy is also proportional to the square of the stress. For a cubic dependency of damping on stress, the logarithmic decrement or the energy ratio plotted linearly versus stress has a straight line proportionality with stress. Van Heydekampf (22), Föppl (8), Hatfield, Stanfield, and Rotheram (2), Contractor and Thompson (13), Kutsay and Yorgiadis (23), and Hanstock and Murray (24), to mention some of the investigators, employed this method of plotting test results. The exact stress relationship is difficult to determine for much of this work, although it appears that for most materials the variation is to an exponent greater than the second power of the stress.

The tendency of the more recent investigators is to use logarithmic scales in plotting the results. Thus Lazan (25) in tension and direct stress tests on plastics using a resonance method, plotted resonance amplification factor versus stress, and indicated an exponent greater than 2. Kutsay and Yorgiadis (23) on a magnesium alloy in torsion and Lazan and Yorgiadis (26)

4

In further tests on plastics in tension used the same resonance method and found an exponent of approximately 3 for both series of tests. Yorgiadis and Robertson (27) in direct stress tests on plywood demonstrated an exponent of approximately 3. Robertson and Yorgiadis (19), plotting damping loss per cycle versus stress to logarithmic scales, present evidence that the variation should be as the third power of stress for a wide variety of materials from plastics to alloy steel. Later work by Sauer and Oliphant (28) on plastics disagreed with the value of 3 for the stress exponent found by the preceeding investigators for a given plastic. They contend that the proper exponent is approximately 2.3. They mention that, considering scatter, this value of exponent fits the data of Robertson and Yorgiadis for this material as well or better than the exponent 3.

To summarize these results, damping tests made in direct stress, flexure, and tension, by temperature rise, rotating beam, decay, and resonance methods, over a considerable range of test frequencies, on both solid and hollow specimens, on a wide variety of materials from wood to alloy steels, indicate that at least in an intermediate stress range, the damping energy varies with stress magnitude to a power in the range of 2 to 3. Whether the exponent is the same for all materials for direct, flexural, and torsional stresses; whether in a given material it varies with the type of test; whether for a given type of stressing it varies with the material; these and others are questions still to be answered by further research.

The sudden rise in damping beyond a certain critical stress, referred to previously in the work of Ludwik, Lehr, Kimball and Lovell, and others, was investigated by Dorey (29) who plotted his results on a variety of steels to logarithmic scales and showed that his damping energy data satisfied exponential relationships with stress both above and below a "quasi-critical" stress for a given material. He found the dissipation to vary approximately as the third power of the stress below and as about the tenth power above the critical stress upon first loading the specimen. For the second loading he obtained a variation approximately as the sixth power above and practically no change in exponent below the quasi-critical stress. Hanstock and Murray (24) show that a very sharp critical stress exists for aluminum alloys above which the damping rises at a rapid rate.

An important deviation from the damping-stress relationship discussed previously for the range below any critical stress, has been noted by several investigators in work on certain ferromagnetic materials. A review of the effect of ferromagnetism on damping is given by Potter (4). A study by Becker and Kornetzki (30) showed that the damping of torsional oscillations in steel wires is reduced to about a tenth by applying a longitudinal magnetic field. Kersten (31) found that the mechanical damping of a ferro-magnetic body is greatly affected if the body is magnetized to a degree below the saturation value. He showed that the damping is due to eddy currents which arise in the oscillating body through variations in magnetization and which are coupled with the mechanical oscillations. The effect of steady and alternating magnetic fields on the damping-stress relationship for two commerical steels is shown by Parker (32) who plotted the dimensionless ratio of damping to elastic energy as a function of stress, linearly. His curves for a Cr-Mo steel display an increase and then a decrease when plotted versus stress. The energy loss was found to be lower at all stresses when a steady field was present and to decrease still further in the presence of an alternating field.

Recent data by Cochardt (33) concerning a high-strength ferromagnetic alloy also indicates a peak in the curve of logarithmic decrement versus torsional stress occurring at an intermediate value of stress when tested in the absence of a magnetic field. With the field, the peak is eliminated and the decrement increases steadily with stress. Cochardt concludes that the energy dissipated for constant stress conditions, by the magnetostrictive effect, which represents the principal source of damping in high-strength ferromagnetic alloys, is found to

5

Increase in proportion to the third power of the stress almost up to some critical value and to remain essentially constant thereafter.

2.7 Effect of Stress History

Among those who studied the effect of stress history upon damping capacity in the higher range of stresses was Ludwik (34) who observed first an increase and then a decrease with number of cycles in the energy dissipation for a Cr-Ni steel subjected to fatigue stressing at constant stress amplitude. He employed a method in which the temperature rise in the specimen is measured. For a carbon steel at the higher stresses he observed a continuous increase in the temperature rise to fracture. In other tests on various steels Ludwik and Scheu (35) observed results similar to that in the Cr-Ni steel. In these, they measured the area of the hysteresis loop after intervals of applied stress cycles. Read (36) observed an increase in the logarithmic decrement for a single crystal of zinc with time of vibration when the strain amplitude was large.

Brick and Phillips (37) and Lazan (25) noted a decrease in damping during the vibration of some aluminum alloys. Stainless steel turbine blades were found by Glikman and Grinberg (38) to have decreased in damping as a result of long service. Wilkes (39) made tests on four gas turbine bucket materials conducted at elevated temperatures. He found that two materials with extremely high initial damping tended to lose a large portion of it with testing time. The other materials showed damping changes of as large as 25 per cent. Both increasing and decreasing trends with stress history were observed. Most of the data were taken below the fatigue strengths. Hanstock and Murray (24) found that an aluminum alloy heat treated to a condition of optimum mechanical properties increased in damping capacity during vibration. Two aluminum alloys containing magnesium, investigated by Hanstock (40), decreased in the ratio of damping to elastic energy until failure occured in constant stress fatigue tests. Other instances of a change in damping properties during high stress fatigue testing have also been reported.

Brick and Phillips (37) studied changes in the damping of Alclad 24ST alloy during the course of fatigue tests. By means of decay tests, they determined the relationship between specific damping and stress after various numbers of cycles at levels above and below the fatigue strength. Fatigue stressing above the endurance limit sharply decreased the damping at high stresses. As failure became imminent, i.e., fatigue cracks were propagated into the core, the damping at low stresses greatly increased. They associated the observed changes with work hardening and cracking.

Hanstock and Murray (24) in explaining the changes in damping of aluminum alloys with continued alternating stressing at a value above a certain critical stress also attribute the changes to strain hardening and fatigue. They associate strain hardening with a gradual decrease and progressing fatigue failure with a gradual increase in damping capacity. They postulate that increase in damping occurs as a result of the formation of fatigue cracks. Although this explanation may be satisfactory for the aluminum alloys, it would appear unable to explain fully such a behavior as an increase in damping followed by a decrease before failure or some of the other complex patterns which have been observed recently in the effect of stress history on damping.

2.8 Damping and Fatigue

Certain of the earlier experiments were performed to determine if the fatigue limit of a material is indicated by a marked change in the damping properties. A review by Vitovec and Lazan (20) summarizes the results of numerous investigators dealing with the relationship of both high and low stress damping to the fatigue properties of a material. Changes in low

6

stress damping as an indication of fatigue are not considered reliable because of the sensitivity of this property to many factors other than fatigue stressing. The review mentioned above, however, does indicate that there may be some connection between the fatigue strength and the sudden increase in damping at a particular level in the high stress region discussed previously.

Among those who considered stress history in the investigation of the relation of changes in damping to fatigue strength were Brick and Phillips (37), Dorey (29), and Hanstock (40). Brick and Phillips found that stress history was a factor in the damping-stress relationship. Dorey also demonstrated this dependence for steels, but showed that for his materials the value of the "quasi-critical" stress was not affected by stress history. The stress at which a rapid increase in damping occurs was found, in general, to be below the fatigue strengths for both ferrous and non-ferrous materials. Foppl (8) indicated this in his work, but pointed out that some specimens withstood many million reversals slightly above the critical deformation point, and so he did not connect it with the torsional fatigue strength. Brophy (41) studied the relation between damping capacity and fatigue, but drew no general conclusions from his test results, saying only that high damping capacity is usually associated with low fatigue limits. This is dependent upon the material, however.

To generalize, a possible association is indicated between changes in high stress damping as a function of stress magnitude and/or stress history and impending fatigue failure, but more work is needed to clarify any such association.

2.9 Damping and Elasticity

In any study of the damping capacity of a material, knowledge of the dynamic stiffness behavior is also desirable. For interpretation of damping data by certain methods of determination, it is necessary to make certain assumptions concerning the nature of the dynamic modulus of elasticity. It is often assumed for this purpose and for other applications that the dynamic modulus has a constant value identical with the static modulus of a material. In general this is not true, for the dynamic modulus of elasticity or the ratio of stress to strain effective during a vibration is usually lower than the static modulus, but may under certain conditions be greater than that value.

Lazan (25) presents a discussion of four main reasons for the deviation between the dynamic and static moduli of elasticity. These are temperature increase caused by damping, hysteresis-loop distortions, cold working, and thermodynamic effects. Because of dissipation of part of the vibrational energy through heat, cyclic stressing of materials may raise their temperature. Since the mechanical properties of materials are a function of specimen temperature, the dynamic modulus of elasticity also deviates from the static value. This factor has only a small influence on the dynamic moduli of metallic materials, but in general an important one in the case of plastics.

A material which displays a curved stress-strain relationship or a significant hysteresis loop in a given stress range does not possess a constant modulus of elasticity. The variation in the tangent or secant modulus during a cycle of stress depends on the area within the hysteresis loop and, therefore, increases with increasing magnitude of stress. The dynamic modulus of elasticity for a given stress cycle, which associates the alternating stress with the corresponding alternating strain, is a mean secant modulus. Materials possessing high damping capacity should have a lower dynamic than static tangent modulus as the stress increases. Due to this factor alone, in metals which show the damping increasing rapidly after a given value of stress, the dynamic modulus should begin to decrease rather sharply at the same point.

7

A third factor affecting the dynamic modulus is the action of the cyclic stress accompanying a dynamic test. In metals this results in cold working of the material which can cause a minor change in modulus of elasticity. In certain alloys, furthermore, the cyclic stress can accelerate the process of natural aging and precipitation, see Hanstock (40), which in some cases may also cause a change in modulus. These effects would probably cause only a relatively small change.

Lastly, the determination of the static load-deflection curve of a material proceeds slowly enough to permit the assumption that the specimen is always at room temperature. The static modulus of elasticity is thus essentially the isothermal value. During cyclic stressing, however, the alternating strains may occur too rapidly to allow thermal equilibrium to be obtained, and the vibration is more nearly adiabatic in nature. This behavior requires the specimen to undergo cyclic temperature changes at the vibration frequency. These temperature changes cause contraction and expansion in the specimen, resulting in the effective or adiabatic modulus being slightly higher than its isothermal value. For most materials, however, the difference between dynamic and static moduli due to this cause is only of the order of one per cent.

In many of the low stress damping capacity or internal friction studies, the variation of the elastic moduli were also determined. However, few of the investigators concerned with high stress damping dealt with the dynamic modulus of elasticity until more recent years. Among those who presented data on the variation of dynamic modulus of elasticity with stress is Lazan (25) who showed that the decrease in the modulus of rigidity with stress for various plastics can be as much as 40 per cent below the static modulus. For an aluminum alloy, however, his data indicated a relatively constant dynamic modulus of elasticity over the stress range investigated. Kutsay and Yorgiadis (23) in torsion tests on two magnesium alloys showed the effect of cold work (number of fatigue cycles at a given stress) on the dynamic modulus of rigidity. Among other observations, they concluded for the materials tested that the damping capacity increases and dynamic modulus of rigidity decreases with increasing stress, and that damping capacity decreases and dynamic modulus of rigidity increases with cold working. Robertson and Yorgiadis (19) obtained data on the variation in the dynamic modulus of elasticity of various materials with stress amplitude. They found that the dynamic modulus of rigidity decreases for SAE X4130 steel and a magnesium alloy as the stress increases. It is significant that the curves are relatively constant for a range of stress amplitudes and then begin to deviate rather sharply downward. This behavior is to be expected in certain cases as mentioned previously. Similar behavior was obtained in the tension-compression dynamic moduli of elasticity for SAE X4130, a magnesium alloy, and bakelite. Little discussion of these results was presented by the authors.

2.10 Elasticity and Fatigue

Few, if any, of the previous investigations have attempted to associate any point on the dynamic modulus versus stress curve with the fatigue limit of a material, but several investigators have noted a possible connection between the fatigue limit of various materials and the dynamic stiffness as evidenced by a dynamic stress-strain or load-deflection curve. The review by Vitovec and Lazan (20) summarizes the work in this field by Smith (42), Gough (43), Kaufmann (44), and Mason (45), among others. The experiments showed, in general, that the dynamic proportional limit is a little higher than the fatigue limit, that it gives approximate values for the fatigue limit for both steels and certain nonferrous metals, but not for aluminum alloys. However, in considering the relationship between the dynamic proportional limit and the fatigue limit, the several factors which affect the proportional limit must be carefully weighed. Among these are strain-hardening effects caused by stress history, effect of strain rate, and as in all proportional limit determinations, the accuracy of testing which affects

significantly the point where nonlinearity is first observed. At present, there is not a very clear picture of the association between dynamic stiffness and fatigue.

III. CHRONOLOGY OF WORK DONE BY THE MINNESOTA GROUP ON

DAMPING, ELASTICITY, AND FATIGUE PROPERTIES

Early work was concerned with the development of new, rotating beam equipment and resonance vibration machines for the study of the damping, elasticity and fatigue properties of materials. An initial study by Lazan (46) described the rotating beam equipment and reported on the dynamic properties of mild steel determined through its use. Test data indicated the changes in damping capacity and dynamic modulus of elasticity of hot-rolled mild steel during a fatigue test. In general, cyclic stress below approximately 80 per cent of the fatigue limit has little effect on damping and elasticity, whereas stress applied between this newly named cyclic stress sensitivity limit and the fatigue limit increased damping as much as 2500 per cent and reduced the modulus as much as 11 per cent. Using equations derived from hysteresis loop relationships, it was shown that the decrease in dynamic modulus of elasticity can be predicted with reasonable accuracy from the increase in damping capacity. Exploratory tests on variable stress histories, overloading, underloading, rest, speed, and other variables were described.

A later investigation by Lazan and Wu (47) more intensively studied the dynamic properties of mild steel at dynamic stress levels in the range from approximately 60 to 120 per cent of the fatigue limit. In this study, as in the previous one, measurements were made on the damping and stiffness properties during the course of fatigue tests at constant stress. Data on the effect of several important test variables such as stress magnitude, history, frequency, and rest were obtained. The existence of a cyclic stress sensitivity limit for the damping properties of mild steel was confirmed. This is a stress below which damping is independent of stress history. For mild steel the location of the cyclic stress sensitivity limit was reported as approximately 80 per cent of the fatigue limit. Above this stress in this material the damping generally increases and the dynamic modulus of elasticity decreases with stress history at a given stress level. Furthermore, a pronounced increase in the rate of change of damping with stress occurs at the cyclic stress sensitivity limit in mild steel.

Dynamic stress-strain relations were also studied in detail in the work on mild steel by Lazan and Wu. They found that the dynamic proportional limit of the virgin specimens was near the fatigue strength of the mild steel. They observed that the damping and dynamic modulus of this material are insensitive to frequency below the dynamic proportional limit, but are dependent on frequency above it. They found that stress history had an effect on the dynamic proportional limit, and the limit decreased with number of stress cycles for stresses above the cyclic stress sensitivity limit. The frequency investigation covered the range from 0.05 to 10,000 cycles per minute. Frequency sensitivity data were also presented in terms of strain rate and flow stress.

The effect of temperature on the dynamic properties of several heat-resistant materials was studied by Lazan and Demer (48) in the high stress region using the rotating beam equipment adapted to elevated temperature studies. Various patterns were observed in the behavior of the damping and elasticity properties during the constant stress tests carried out at engineering stress levels at room and various elevated temperatures. For all materials and at

all temperatures investigated, the energy dissipated by damping increased rapidly with stress at values close to the fatigue strength of a material. Cyclic stress sensitivity limits were not determined for these materials; all the tests were carried out at higher stresses. Exponents for the variation of damping with stress determined from the results of these tests varied for the different materials at the different temperatures from values as low as approximately 2 to as high as 25 in one case.

Various patterns were observed by Lazan and Demer in the variation of damping during a reversed cyclic stress test at a given level. Depending upon the material and the temperature, the damping energy may decrease, remain the same, increase, or have a complex pattern of increase and decrease, or decrease and increase, as the number of stress cycles is increased. There was no regular behavior for all materials, and changes of substantial magnitude were found to take place at stresses below the fatigue strengths. In general, the changes in dynamic modulus of elasticity were reciprocal to the changes in damping energy. All of the damping and elasticity readings were taken at a frequency of 20 cycles per minute, and no effect of frequency was investigated.

A more detailed study of the effect of temperature on the dynamic properties of a particular material was made by Demer and Lazan (49), (50) using the heat-resistant alloy N-155. This material was investigated at three temperatures: room, 1350 F, and 1500 F over a wider stress range than in the study just described. The results revealed the existence of a cyclic stress sensitivity limit for damping at all three temperatures with roughly similar damping-stress relationships for unnotched specimens. The cyclic stress sensitivity limit occurred between approximately 65 and 85 per cent of the fatigue strength at a given temperature. Damping was found to vary nearly as the cube of the stress magnitude at all three temperatures for stresses below the cyclic stress sensitivity limit. Beyond that stress, the damping curves at all three temperatures were again approximately linear on a log damping versus log stress plot, but with much steeper slopes in most cases. The slopes were in the range of from 4 to 10, with the value depending on the stress history and temperature. At 1500 F, stress history had only a small effect on damping above the cyclic stress sensitivity limit; at 1350 F, the damping decreased with stress history; and at room temperature, both increasing and decreasing tendencies were observed depending on the level of stress above the cyclic stress sensitivity limit.

Changes in the dynamic modulus of elasticity of N-155 were also noted in the work by Demer and Lazan. The curves of dynamic modulus versus stress showed that at 1350 F and room temperature there was a pronounced decrease in modulus beginning at stresses roughly 70 - 75 per cent of the fatigue strength, but at 1500 F the dynamic modulus changed little up to the fatigue strength. At higher stresses there was an initial decrease followed by a measureable increase in dynamic modulus as a result of stress history.

Tests were also made on N-155 using notched specimens. With these, up to the point where cracking occurred during the fatigue test, stress history had no effect on damping or stiffness even at the highest stress employed. The exponent of the log damping versus log stress relationship for the notched specimens was approximately the same at all three temperatures, 3.6.

An association between the dynamic proportional limit and the fatigue strength of N-155 at the three test temperatures was sought in this study. At 1500 F the fatigue strength of the unnotched specimens was very close to the dynamic proportional limit, whereas at the other two temperatures it was at a stress approximately 20 per cent above the proportional limit. Other portions of the study included work on the detection of cracking in the notched specimens, analysis of the stiffness characteristics of notched specimens, and investigation of the rotating bending fatigue notch sensitivity at the three temperatures.

Recently, Vitovec and Lazan (52), (53) have reported data on the damping, elasticity, and fatigue properties of 24S-T4 aluminum alloy and mild steel under progressively increasing cyclic stress.

IV. SPECIFIC OBJECTIVES OF INVESTIGATION

Determination of the generality of certain of the observations made in the previous work on mild steel and the heat-resistant alloys, and possible explanation for the behaviors noted were chosen as the next phase of the broad investigation at the University of Minnesota. It was decided to apply the rotating beam damping, elasticity, and fatigue tests, at room temperature, using a fixed frequency for the damping and elasticity observations, to materials of various types, extending the tests over a wide range of stress to determine, if possible, any general laws of behavior which may exist. By careful control of various factors found to affect damping and dynamic modulus it was hoped to uncover inconsistencies in the results of some previous investigators as well as to clarify any generalized behavior trends in the work of others. Work reported herein is confined to the properties under sustained cyclic stress of constant magnitude.

The specific objectives of this investigation of a group of various metallic engineering materials were:

(a) to study the variation of damping and dynamic modulus with stress history over a wide range of stress magnitudes;

(b) to investigate the generality of the existence of a cyclic stress sensitivity limit as observed for SAE 1020 steel (47);

(c) to compare the relative damping and stiffness properties of the various materials;

(d) to correlate the changes in damping with the changes in dynamic modulus; and

(e) to discover any possible relationship between the damping or stiffness properties and the fatigue strengths.

Investigation of the effect of frequency on the dynamic properties of materials is not covered in this paper.

11

V. EXPERIMENTAL PROGRAM

5.1 Test Materials

Materials chosen for this study were gray cast iron; Sandvik steel, a high carbon material, in both the normalized and the quenched and tempered conditions; N-155, a heat-resistant alloy; 24S-T4 aluminum alloy; J-1 magnesium alloy; and SAE 1020 steel, for comparison purposes. This selection was made to provide a variety in types as well as to cover a wide range of fatigue strengths.

Details on the chemical composition, processing, and thermal treatment of the materials are given in Table I. The static physical properties obtained in standard tension tests are reported in Table II. These values are the average of two or more tests. In preparing the Sandvik steel materials it was intended to obtain both the normalized and the quenched and tempered blanks with the same hardness. This goal was not exactly achieved; the BHN for the normalized pieces was approximately 365 and for the quenched and tempered lot, 415.

5.2 Test Specimens

Unnotched cylindrical test specimens of the type shown in Fig. 1 were used in this work. In the figure are given the dimensions of the specimens used for each material. Various specimen sizes were used in order that the required loads might be within the limitations of the testing machines. The specimens were tapered so that under the cantilever loading imposed by the machine, the outer surface of the entire length of the test section would be subjected to the same peak stress.

All specimens were carefully prepared so as to assure a smooth specimen surface free from cold work and internal stress. The specimens were machined and then polished with successively finer abrasives in such a way that fine scratches remaining were in a longitudinal direction. For additional details on the preparation of the unnotched specimens see Appendix A. The specimens were not given any thermal treatment after machining.

5.3 Test Equipment

Recent publications (46), (47) have given detailed descriptions of the rotating cantilever equipment employed in performing the fatigue tests. The methods for determination of the damping and elasticity properties from readings taken during the course of such constant stress tests are explained in detail in Appendix B of this report.

5.4 Test Procedure

Each of the seven materials was tested in the rotating beam damping, elasticity, and fatigue machines. Damping energy and dynamic modulus of elasticity were measured at intervals during each constant stress magnitude fatigue test. Several stress levels in the vicinity of the fatigue limit or the long time fatigue strength were used to determine the S-N curve. Tests above the fatigue limit were carried to fatigue fracture, whereas tests below the fatigue limit were continued, in most cases, until the damping energy did not change significantly with number of stress cycles. For damping data in the low stress range, one or two specimens of each material were used to obtain damping values at several different stress levels.

The general procedure for conducting the constant load rotating cantilever beam fatigue tests has been described in previous publications (46), (47), (48) and will be omitted here. It should be noted, however, that all of the readings for damping and elasticity were taken at 20 rpm. Various testing speeds in the range from 20 to 1500 rpm were used between

readings in the course of the fatigue tests for different periods in the life of a specimen in order to keep the lower stress tests to a reasonable duration.

VI. EXPERIMENTAL RESULTS

6.1 Fatigue Properties

Conventional S-N fatigue curves for all materials tested in this study are shown in Fig. 2. Stress is plotted to a logarithmic scale to facilitate comparison of the materials with widely different fatigue properties. The plotted points represent cycles to complete fracture. The fatigue strengths at 2×10^7 cycles, as determined from these curves, are given in Table II. It should be noted that relatively few specimens were used for each curve, that specimens of different diameters were tested for the various materials, and that the testing speed employed varied in the range from 20 to 1500 rpm. Obviously, the gray iron tested was not of a high strength, but no attempt was made to secure the optimum material in each class for these tests.

6.2 Damping Properties

Deflection measurements made on a target in the end of the loading arm attached to the rotating beam specimen, upon reversal of direction of rotation, provide data for determining the total damping energy in in-lb per cycle being dissipated in the entire specimen. Since the test section is subjected to rotating bending conditions, the stress varies from zero at the center to a maximum at the outer periphery. Thus, total damping energy is not a basic measurement of damping energy since it depends on the type of specimen and the stress distribution. Furthermore, the total damping includes also the energy dissipation in the fillets.

The data of Fig. 3, for one of the materials, are presented to show the type of original data obtained in these tests. In this figure, each curve shows the damping data obtained during a fatigue test on a single specimen. It is to be noted that the damping is unaffected by number of cycles below a certain value of stress. Above this limiting stress the damping changes significantly even in those specimens which did not fail in more than 30 million cycles of stress.

For the other materials investigated, different patterns for the damping behavior were obtained as shown in Fig. 4. Due to space limitations, the original observations have been omitted from this figure and only the curves themselves are shown. One characteristic common to all of these materials is that in the lower stress ranges, the damping is unaffected by stress history. This indicates a cyclic stress sensitivity limit for each of the materials tested.

Above the cyclic stress sensitivity limits the materials display no general similarity of behavior in regard to the manner in which the damping changes with stress history. In the case of 1020 steel, as with the quenched and tempered Sandvik steel, sustained cyclic stress of constant magnitude gradually increases the damping up to the point of failure or to a point where damping becomes stabilized. For the aluminum alloy and gray iron the reverse occurs; the damping is decreased by sustained cyclic stress. For the normalized Sandvik steel and the J-1 magnesium alloy the cyclic stress causes first an increase and then a decrease in the damping. Such dissimilarity as the above, and even still different patterns were previously noted (40) for heat-resistant materials in the high stress region. Although, in most cases, the general pattern of change for a given material is independent of stress level, this is not always true. For example, with N-155 at stresses above the cyclic stress sensitivity limit but below

about 110 per cent of the fatigue limit, cyclic stress causes a decrease in damping, whereas, at higher stresses the reverse is true.

In Appendix B of this paper a method is described for converting the total damping energy data presented in Figs. 3 and 4 to specific damping energy. As used here, specific damping energy is the energy absorbed per cubic inch of material under conditions of uniform direct stress. It is the damping associated with a given unit stress and is expressed in in-lb per cu in. per cycle.

Specific damping energy data for the various materials are shown in Fig. 5 in the form of a log-log diagram as a function of stress. The values in the high stress ranges were determined from data shown in Fig. 4. For the lower range of stress, considerably below the cyclic stress sensitivity limit, the damping data were obtained by testing individual specimens at various stress levels. This procedure is valid since in this range there is no effect due to stress history.

All of the rotating beam damping and elasticity data were obtained at 20 rpm. The previous investigation of mild steel (47) showed no frequency effect in the range below the cyclic stress sensitivity limit. A few exploratory tests, however, indicate in the case of some other materials, notably magnesium and aluminum, that important frequency effects may exist below the cyclic stress sensitivity limit. It is important to remember that these results and the relative properties of these materials are only for the frequency of 20 cycles per minute. The effect of frequency on the dynamic properties of materials will be reported in a subsequent paper.

There are several important characteristics of the results shown in Fig. 5 which should be emphasized. First, as previously noted, apparently all of the materials tested display a cyclic stress sensitivity limit for damping. For the magnesium and aluminum alloys, the cyclic stress sensitivity limit is not sharply defined. The accuracy of its determination depends largely on the number of specimens tested in that stress range and upon the scatter in the damping data. For gray iron, stress history has the smallest effect of any of the materials shown. In the high stress range with this material there are only relatively small changes in damping due to this factor. The location of any definite cyclic stress sensitivity limit for this material is therefore difficult. The cyclic stress sensitivity limit shown in Fig. 5 for this material is an approximate value determined from the solid specimen test results. The location of this stress for the magnesium and aluminum alloys is more reliable than for gray iron, but still not so precisely determined as in the case of the other ferrous materials where the rate of change of damping with stress is much more pronounced at the cyclic stress sensitivity limit. The approximate stress values at these points are given in Table II along with the ratio of this stress to the fatigue strength at 2×10^7 cycles for each material. The ratios vary from 0.5 for J-1 magnesium to 1.1 for the quenched and tempered Sandvik steel. The latter case is the first one noted where the cyclic stress sensitivity limit falls above the fatigue strength. The values of specific damping energy for the various materials at the cyclic stress sensitivity limit are given and they range from 2.8 in-lb per cu in. per cycle for quenched and tempered Sandvik steel to 0.095 in-lb per cu in. per cycle for J-1 magnesium. It is interesting to note that 1020 steel and the aluminum alloy have very nearly the same values for stress ratio at the cyclic stress sensitivity limit and also for damping energy at that point.

A second important feature of Fig. 5 which should be observed is that for each material the slope of the log specific damping energy versus log stress relationship is constant below the cyclic stress sensitivity limit in the stress range investigated, as far as the rotating beam method of damping determination is able to ascertain. This method, it is true, is clearly limited in the low stress range of damping measurements due to the extremely small horizontal

14

displacement readings encountered. Approximate scatter bands for the single specimen tests for each material in the range below the cyclic stress sensitivity limit are shown in Fig. 5. The reason for the uncertainty of the location of this point for gray iron and the aluminum and magnesium alloys in which the damping change at that point is not abrupt is obvious from examination of this figure.

It should be recalled that dissipation of energy due to magneto-elastic effects as discussed by Potter (4), Parker (32), and Cochardt (33), may result in certain ferromagnetic materials displaying a damping peak or plateau in the lower stress range when tested in the absence of a magnetic field. Such behavior would be contradictory to that shown in Fig. 5 for the alloys tested. If such behavior is characteristic of the ferromagnetic materials tested in this program it was of too small a magnitude, or occurred at too low a stress to be detected by the rotating beam machine. Of course, no such behavior would be possible in the case of the nonferrous materials tested.

The slope values for the logarithmic damping-stress curves in Fig. 5 are given in Table II. Difficulty in obtaining reliable damping readings by the rotating beam method in the lowest stress range would make these values of slope somewhat questionable. They were, however, checked by data obtained on a vibration decay damping machine currently being developed. For each material there was close agreement between the slope values obtained by the two methods. The values were as follows: normalized Sandvik steel, 2.6; N-155, 2.5; gray iron, 2.4; quenched and tempered Sandvik steel, 2.3; and 2.0 for 1020 steel, 24S-T4 aluminum, and J-1 magnesium. The value shown for N-155 is lower than the value of 3.0 given in previous publications (49), (50). This results from further vibration decay tests being carried out on this material over a wider stress range than in the earlier investigation. The straight line portions of the data for the various materials, of course, indicate that the damping energy increases as a power function of the stress. Thus, in the region below the cyclic stress sensitivity limit the relationship may be shown as:

$$D = J S^n$$

where D = specific damping energy

S = stress amplitude

J, n = constants (values for n were given in the above paragraph)

The slope or exponent values obtained in this study are not in exact agreement with the conclusion of Robertson and Yorgiadis (19) who, as previously mentioned, found that the damping capacity of engineering materials under both shearing and normal stresses below the yield strength and for completely reversed stress is directly proportional to the third power of the stress amplitude. Their values were obtained at higher frequencies (approximately 10 to 70 cycles per second) than the data of the present investigation. However, they further concluded that the damping capacity of materials is independent of the frequency of stressing.

Except for gray iron, the rate of change of damping with stress above the cyclic stress sensitivity limit is much greater for the ferrous materials than for aluminum and magnesium. The most rapid increase in damping above the cyclic stress sensitivity limit is displayed by 1020 steel and the normalized Sandvik steel. In Table II are given the range of exponents or slopes of straight lines on the logarithmic damping-stress plot which approximate the curves for the various materials in the high stress ranges. Gray iron exhibits the lowest values with a maximum of roughly 3, whereas 1020 steel indicates relationships approaching an exponent of approximately 21 for certain of the curves for equal stress history. Above the cyclic stress

sensitivity limit, stress history has the greatest effect on the damping of the quenched and tempered Sandvik steel, 1020 steel, and aluminum in the high stress range. The effect of repeated cycles of stress is the least in the case of N-155 and gray iron.

6.3 Comparison of Damping Properties

When compared on an equal stress basis in the range below the cyclic stress sensitivity limits, gray iron displays the greatest damping ability with magnesium, aluminum, and 1020 steel following in that order. It is to be noted that on this basis of comparison in the region below that in which stress history has an effect, the damping capacity is approximately inversely proportional to the fatigue strengths of the material.

A method of comparing the relative damping properties of materials while recognizing their different fatigue strengths is shown in Fig. 6a which uses as an abscissa the logarithm of the ratio of test stress to fatigue strength. On this basis of comparison the order of the different materials is changed from that of Fig. 5. In the low stress region the high carbon steel in both conditions of heat treatment displays greater damping than gray iron which is still superior to the other materials. At the stress ratio of one the damping energy is dependent upon stress history, but in general all of the materials except aluminum and magnesium display greater damping after a long stress history than does gray iron. The damping values at the cyclic stress sensitivity limits for the various materials and the range of damping at the fatigue strength are given in Table II.

In Fig. 6a, the data for all of the materials tested fall in a relatively narrow band in the range below the cyclic stress sensitivity limits. Equations of the approximate limits for this band are:

$$D = 3.0 \ R_f^{2.5} \quad \text{(upper limit)}$$

$$D = 0.4 \ R_f^{2.0} \quad \text{(lower limit)}$$

where R_f = the ratio of test stress to fatigue strength at 2×10^7 cycles

D = specific damping energy in in-lb per cu in. per cycle

This band satisfies the data of Fig. 6a over the range of ratios from 0.1 to 0.7.

The effect of the heat treatment on the behavior of the Sandvik steel is interesting. When plotted as in Fig. 6a, the data show similar damping properties in the lower range of stress. Since the cyclic stress sensitivity limit is below the fatigue limit for the normalized material and above it for the quenched and tempered material, it is seen that the damping at a ratio of stress to fatigue strength of 1.0 is much greater for the normalized material.

A comparison of the damping properties which takes into account the different stiffness properties of the materials is shown in Fig. 6b. Here, the specific damping is plotted for each material as a function of strain at the outer fibers. For equal strain values of less than 0.001 in. per in., gray iron is seen to dissipate a greater amount of energy than any of the other materials. The magnesium alloy dissipates the least energy for a given unit strain in this region. Values of unit strain for the different materials at the cyclic stress sensitivity limit and at the fatigue strength at 2×10^7 cycles are included in Table II. The narrowness of the band for the normalized Sandvik steel in Fig. 6b, as compared with that in Fig. 6a, is due to the fact that for this material, the curve for a stress history of 20 cycles was omitted in

16

the plot of damping as a function of strain because of insufficient deflection data.

From the comparisons of the damping properties presented, it appears that rating materials as to their ability to dissipate vibrational energy at engineering stress levels must include consideration of stress magnitude, fatigue strength, and stiffness. A bold statement that one material has higher damping than another is seen to be rather meaningless without consideration of the above factors. Failure to consider them has probably been a reason for the many conflicting opinions and reports found in the literature regarding the relative damping of various materials.

6.4 Elasticity Properties

Dynamic stress-strain curves in bending as obtained from the vertical deflection readings taken during the fatigue tests are given in Fig. 7. Thus, the curves shown for each material are the composite of the results from many different specimens. The strain scale was obtained in each case by comparing the initial portion of the dynamic bending curve with the initial portion of the static stress-strain tension curve and assuming no difference between the static modulus and the dynamic modulus in this range. The materials displaying the greatest deviation from linearity are gray iron, 1020 steel, N-155, and the normalized Sandvik steel; except for gray iron, however, the significant deviations occur only at stresses above the fatigue strength in each case. Values for the approximate dynamic proportional limits are given in Table II. These values were taken from a large scale working plot and therefore were determined more closely than is possible from Fig. 7.

Aluminum and magnesium display only small deviations from linearity up to stresses approximately twice the fatigue strength in each case. The quenched and tempered Sandvik steel also shows little deviation from linearity up to stresses about 50 per cent above the fatigue strength. The most pronounced stress history effect on stiffness is displayed by the 1020 steel and the least by the J-1 magnesium alloy.

The deflection data obtained during the rotating beam fatigue tests may be converted to values of average secant dynamic modulus of elasticity by use of the formulae given in Appendix B. They are called 'average' values because they are determined from values of deflection obtained from bending tests in which only the outer fibers are stressed to a maximum. These values for modulus of elasticity, expressed in per cent of each material's initial static tangent modulus, are plotted in Fig. 8a as a function of maximum reversed bending stress. In Fig. 8b they are plotted as a function of the ratio of cyclic stress to fatigue strength at 2×10^7 cycles. The various fatigue strength values are indicated in Fig. 8a, and the damping cyclic stress sensitivity limits are shown in both figures. Values for the ratio of the approximate dynamic proportional limit to the fatigue strength and to the damping cyclic stress sensitivity limit for each material are given in Table II.

The points shown in Fig. 8 for the start of the stress history effect on dynamic modulus do not correspond closely with the values given in Table II for the approximate dynamic proportional limit in the case of gray iron, J-1 magnesium, and 24S-T4 aluminum. This may be a real effect or merely a result of scatter caused by the limitation of instrument sensitivity or the use of different specimens to obtain the curve for each material. For the above materials, for which the increase of damping with stress at the cyclic stress sensitivity limit is not pronounced, the initiation of stress history effect on dynamic modulus is also difficult to determine. The points shown are therefore only approximate.

It is interesting to consider possible changes in the shape of the hysteresis loop due to cyclic stress. A detailed discussion of the dynamic stress-strain characteristics of mild

17

steel, the same lot as used in these tests, is given in a previous paper by Lazan and Wu (47). In that paper they present the results of tests illustrating the dependence on stress history of the static proportional limit, the dynamic proportional limit, and other dynamic characteristics. They show for this material:

A. Below the cyclic stress sensitivity limit:
1. Both the static and dynamic stress-strain curves coincide.
2. Both are independent of stress history.
3. Neither the static nor the dynamic proportional limit is reached.

B. Between the cyclic stress sensitivity limit and the fatigue limit:
1. Both the static and dynamic stress-strain curves coincide for the virgin specimen.
2. Neither the static nor dynamic proportional limit is reached for the virgin specimen.
3. Under sustained cyclic stress:
   (a) Both the static and dynamic proportional limit decrease, the former more than the latter.
   (b) The static and dynamic stress-strain curves gradually deviate from each other.
   (c) In spite of these changes, the initial tangent modulus of elasticity remains unchanged.

C. Above the fatigue limit, the behavior is similar to, but more pronounced, than that discussed under "B" above, and in addition:
1. The dynamic proportional limit of the virgin specimen is near the fatigue limit.
2. The tangent modulus at zero stress does not remain constant, but gradually decreases under sustained cyclic stress.

Due to the similarity in the damping and elasticity behavior between normalized Sandvik steel and 1020 steel it might be expected that similar changes to those outlined above would also occur with the normalized higher carbon steel. N-155 is similar to the above two materials in that the damping cyclic stress sensitivity limit and the start of the stress history effect on the dynamic modulus of elasticity were found to occur at approximately the same stress, and both are below the fatigue strength. Of course, the cyclic stress sensitivity limit is not at the identical stress for these materials nor at the same ratio of stress to fatigue strength. Sandvik steel in the quenched and tempered condition would seem to possess singular dynamic stress-strain characteristics, for although stress history begins to exert measureable effect on both damping and dynamic modulus at approximately the same stress, this occurs above the fatigue limit. This was not observed in any other material tested. For the magnesium and aluminum alloys the approximate dynamic proportional limits occur quite far above the values determined for the cyclic stress sensitivity limits, but the dynamic proportional limit is above the fatigue strength in the case of the aluminum alloy and below the fatigue strength in the case of the magnesium alloy. The difficulties in determining the cyclic stress sensitivity limits and the dynamic proportional limits for these materials make these points somewhat questionable. It would appear desirable in the future to perform the same type of dynamic stress-strain study on the other materials as was carried out by Lazan and Wu with 1020 steel.

The values of dynamic modulus of elasticity which were discussed above are called 'average' values because, as explained previously, they were determined values of

deflection taken from a bending test in which only the outer fibers are stressed to a maximum. In a direct stress test, where the whole specimen cross-section is at the same stress, it is expected that the deviations of the dynamic modulus of elasticity from the static modulus would be even more abrupt than the behavior shown in Fig. 8. Such values might be called the 'specific' dynamic moduli of elasticity. Work is in progress on methods for determining such specific values from bending deflection data obtained with solid specimens as used in these tests. In the future, specific rather than average dynamic modulus data will probably be reported.

6.5 Relationship Between Damping and Other Physical Properties

As pointed out in the review by Potter (4), attempts have long been made to correlate damping capacity with such other physical properties as hardness, impact resistance, tensile strength, and fatigue resistance. These have been generally unsuccessful except that in any one steel the damping capacity has been found to vary inversely with tensile strength and fatigue strength, Brophy (41).

The difficulty in finding any such general correlation for a variety of materials is probably due to the dependence of the damping property on so many different factors such as stress magnitude, stress history, testing frequency, temperature, grain size, magnectic fields, heat treatment, etc. Since the effects of these variables may be dissimilar in different materials, it is probably of little value to seek any single property with which to correlate damping. An approximate relationship is better than none at all, however, so an attempt was made at such a correlation.

In Table II are given specific damping energy values for the various materials read from Fig. 5 at a stress of 6000 psi, from Fig. 6a at a stress ratio of 0.4, and from Fig. 6b at a unit strain of 0.004 in. per in. In each case these abscissa values were chosen so as to fall below the cyclic stress sensitivity limits for all the materials. The first set of values compares the damping of the materials at constant stress; the second, at constant ratio of test stress to fatigue strength; and the third, at constant strain.

The three sets of values so obtained were plotted using logarithmic scales versus the tensile strength, yield strength, fatigue strength, approximate dynamic proportional limit, stress at the cyclic stress sensitivity limit, and static modulus of elasticity, in seeking a correlation. There is apparently no reasonable association between the damping at constant strain and any of these six parameters. Using the other methods of comparison, approximate correlations were noted for two of the parameters. For the seven materials tested, the data for specific damping at equal stress plotted on this log-log basis were found to satisfy approximate straight lines both as a function of tensile strength and also fatigue strength. In each case, the damping increased with a decrease in strength as shown in Fig. 9. If the same shape is assumed for all of the hysteresis loops, then the width of the loop is greatest for the material of lowest tensile strength. The data for the damping of the materials at a constant ratio of test stress to fatigue strength plotted on a log-log basis as a function of fatigue strength, Fig. 9a, or tensile strength, Fig. 9b, satisfy approximate straight lines except for gray iron. The data for this material fall above the curves for the other materials. On this basis of stress ratio, the damping increases with fatigue strength or tensile strength. The behavior indicates that, even though the width of the hysteresis loop is narrow for the materials of high tensile strength, greater areas are obtained due to the greater height of the loops.

VII. SUMMARY AND CONCLUSIONS

The results of this investigation concerned with the rotating bending fatigue, damping, and elasticity properties of several metallic materials elicit the following observations (all damping and elasticy measurements were made at 20 rpm):

1. Within the sensitivity of the rotating-beam method for the measurement of damping in the lower range of stresses, the variation of specific damping energy with stress satisfies the equation:

$$D = J S^n$$

where: D = the specific damping energy,

S = the maximum value of alternating stress, and

J and n = constants depending on the material.

2. The law given above applies for each material tested in the range below a certain critical stress named the cyclic stress sensitivity limit.

3. Below the cyclic stress sensitivity limit, stress history has no observable effect on damping, while above it, the damping energy is dependent on the stress history. Curves are presented to show the variation of specific damping energy with constant cyclic stress history.

4. For all the materials tested, the value of the exponent n obtained from rotating beam data and checked by a vibration decay method varies between 2.0 and 2.6 in the range below the cyclic stress sensitivity limit. This is somewhat lower than the value of 3.0 reported by several investigators.

5. Above the cyclic stress sensitivity limit, the rate of change of damping with stress increases abruptly for certain materials, particularly the steels and the heat-resistant alloy; the change is somewhat less marked in the aluminum alloy, and it is least in the magnesium alloy and in gray cast iron.

6. If the relationship given under 1. between damping and stress is used to fit roughly the curves above the cyclic stress sensitivity limit, values of the exponent n are found as high as 20 in the case of 1020 steel.

7. There is no consistent pattern of change in damping above the cyclic stress sensitivity limit for all of the various materials when tested under constant cyclic stress. There is a tendency for the damping as a function of stress history to increase in the case of the steels and to decrease in the case of gray iron and the nonferrous materials. Both effects are noted with N-155 at various stress levels.

8. The ratio of stress at the cyclic stress sensitivity limit to the fatigue strength is not constant for all of the materials. It varies from approximately 0.5 for the magnesium alloy to 1.1 for the Sandvik steel in the quenched and tempered condition. For the other five materials tested it falls between

20

0.8 and 0.9. Accurate location of this point is difficult for gray iron and the nonferrous materials due to scatter in the data at the lower stresses.

9. The relative damping properties of the various materials tested depend upon the manner in which they are compared. In the listing given on the next page the test materials are ranked in the order of highest damping for four different bases of comparison (1,2,3,...indicate decreasing magnitude of damping):

Order	Equal Stress Below CSSL	Equal Ratio of S/FS Below CSSL	Equal Strain Below CSSL	Damping at FS
1	Gray Iron	Sandvik (N)	Gray Iron	Sandvik (N)
2	J-1 Mg	Sandvik (Q-T)	1020	N-155
3	24S-T4 Al	Gray Iron	N-155	1020
4	1020	N-155	Sandvik (N)	Sandvik (Q-T)
5	N-155	1020	Sandvik (Q-T)	Gray Iron
6	Sandvik (N)	24S-T4 Al	24S-T4 Al	24S-T4 Al
7	Sandvik (Q-T)	J-1 Mg	J-1 Mg	J-1 Mg

One possible cause for the disagreement of various investigators on the relative ratings of various materials is the use of different bases of comparison. A second cause is the failure to control significant test variables in the experimental work.

10. The values for dynamic proportional limit in rotating bending have no consistent relationship to the fatigue strengths, the damping cyclic stress sensitivity limits, or the static tensile strengths for all materials tested. For the steels and N-155 the dynamic proportional limit falls within 20 per cent of the damping cyclic stress sensitivity limit. For the nonferrous materials the dynamic proportional limit is apparently above the cyclic stress sensitivity limit. In noting these observations it should be remembered that the values obtained for the dynamic proportional limit are for several reasons only approximate.

11. At their respective fatigue strengths, none of the materials, with the exception of gray iron, exhibits an average dynamic modulus of elasticity lower than 95 per cent of its static modulus. For gray iron the dynamic value is approximately 10 per cent below the static value. Data in this paper on solid specimens of mild steel show a decrease in average dynamic modulus of only 5 per cent at the fatigue strength. Tests on hollow specimens of the same material (47) show a corresponding decrease in average dynamic modulus of 11 per cent. The decrease in specific dynamic modulus, which might be obtained from direct stress tests where the whole specimen cross-section is at the same stress, would be even greater.

12. The nonferrous materials suffer little change in their stiffness properties when subjected to stresses well above their fatigue strengths. Their dynamic moduli of elasticity are the least affected by stress history of any of the materials tested.

13. The data for the damping energy D in in-lb per cu in. per cycle for all materials tested, plotted as a function of the ratio of test stress to the fatigue strength at 2×10^7 cycles R_f, are satisfied by a band the limits of which are given by the lines:

$$D = 3.0 \, R_f^{2.5}$$

$$D = 0.4 \, R_f^{2.0}$$

This band satisfies the data in the range of ratios from 0.1 to 0.7.

14. A comparison of the relative damping properties for equal stress below the cyclic stress sensitivity limits indicates that the damping energy decreases with an increase in the fatigue and tensile strengths of the various materials. The damping energies compared on the basis of equal ratio of stress to fatigue strength show an increase with both the fatigue and tensile strengths. On this basis, gray iron displays a damping energy far above curves satisfying the data for the other materials tested.

BIBLIOGRAPHY

(1) A. L. Kimball, "Vibration Problems, Friction and Damping in Vibrations," Parts IV and V. Journal of Applied Mechanics, March 1941, pp. A-37 to A-41, September 1941, pp. A135 to A140.

(2) W. H. Hatfield, G. Stanfield, and L. Rotherham, "The Damping Capacity of Engineering Materials," Trans. N. E. Coast Institution of Engineers and Shipbuilders, Vol. 63, pp. 273-332 (1942).

(3) F. C. Thompson, "Damping Capacity," British Non-Ferrous Metals Research Association, Report No. 657, August 1944.

(4) E. V. Potter, "Damping Capacity of Metals," U. S. Dept. of Interior, Bureau of Mines, Report of Investigations No. 4194, March 1948.

(5) E. Linacre, "Damping Capacity," Iron and Steel, Vol. 23, pp. 153-156, 285-288, 344-348 (1950).

(6) A. W. Cochardt, "A Method For Determining the Internal Damping of Machine Members," Westinghouse Scientific Paper, No. 172i, Westinghouse Research Laboratories, East Pittsburg, Pa., 29 January 1953.

(7) B. J. Lazan, "Damping Constants and Stress Distribution in Resonance Response," Journal of Applied Mechanics, Vol. 20, No. 2, pp. 201-209 (1953).

(8) O. Föppl, "The Practical Importance of the Damping Capacity of Metals, Especially Steels," Journal of the Iron and Steel Institute, Vol. 134, pp. 393-423 (1936).

(9) C. Zener, "Internal Friction In Solids," Proc. Phys. Soc., Vol. 52, pp. 152-156, 1st Jan. 1940.

(10) A. S. Darling, "Internal Friction Measurement," Metal Industry, Vol. 78, pp. 223-225, 271-273, 291-292 (1951).

(11) C. Zener, "Elasticity and Anelasticity of Metals," The University of Chicago Press, Chicago, Ill. (1948).

(12) K. Bennewitz and H. Rötger, "On the internal Friction of Solid Bodies; Absorption Frequencies of Metals in the Acoustic Region," Physikal Z. 1936,37 (16), pp. 578-588.

(13) B. Hopkinson and G. T. Williams, "Elastic Hysteresis of Steel," Proc. Roy. Soc., A, Vol. 87, pp. 502-511, Dec. 13, 1912.

(14) F. E. Rowett, "Elastic Hysteresis in Steel," Proc. Roy. Soc., A, 89, pp. 528-543, March 2nd 1914.

(15) A. L. Kimball and D. E. Lovell, "Internal Friction In Solids," Phy. Rev. Vol. 30, pp. 948-959 (1927).

(16) A. Gemant and W. Jackson, "Internal Friction in Solid Dielectrics," Phil. Mag. 23, pp. 960-983, May 1937.

(17) A. Gemant, "The Measurement of Solid Friction of Plastics," Journal of Applied
Physics., Vol. 11, pp. 647-653 (1940).

(18) G. P. Contractor and F. C. Thompson, "Damping Capacity of Steel," Journal, Iron
and Steel Inst., V. 141, pp. 311-217 (1940).

(19) J. M. Robertson and A. J. Yorgiadis, "Internal Friction in Engineering Materials,"
Journal of Applied Mechanics, June 1946, pp. A173-A182.

(20) F. H. Vitovec and B. J. Lazan, "Review of Previous Work On Short-Time Tests For
Predicting Fatigue Properties of Materials, WADC Technical Report No. 53-122,
April 1953.

(21) W. Spaeth, "Physik der mechanischen Werkstoffpruefung," Springer, Berlin, p. 164,
1939.

(22) G. S. von Heydekampf, "Damping Capacity of Materials," Proceedings, Am. Soc.
Testing Mats., Vol. 31, part II, pp. 157-175 (1931).

(23) A. U. Kuteay and A. J. Yorgiadis, "On the Torsional Damping Capacity of Solid
Magnesium Alloy Rods as Affected by Cold Working," Journal Aero. Sci., Vol. 10,
No. 8, pp. 303-310 (1943).

(24) R. F. Hanstock and A. Murray, "Damping Capacity and the Fatigue of Metals,"
Journal of the Institute of Metals, Vol. 72, pp. 97-132 (1946).

(25) B. J. Lazan, "Some Mechanical Properties of Plastics and Metals Under Sustained
Vibrations," Transactions, Am. Soc. Mechanical Engrs., Vol. 65, pp. 87-104 (1943).

(26) B. J. Lazan and A. J. Yorgiadis, "The Behavior of Plastics Under Repeated Stress,"
ASTM Symposium on Plastics, p. 91, 1944.

(27) A. J. Yorgiadis and J. M. Robertson, "Plywood Characteristics Disclosed by Vibration
Tests," Aero Digest, April 1, 1944.

(28) J. A. Sauer and W. J. Oliphant, "Damping and Resonant Load-Carrying Capacities
of Polystyrene and Other High Polymers," Transactions Am. Soc. Testing Mats.,
V. 49, pp. 1119-1131 (1949).

(29) S. F. Dorey, "Elastic Hysteresis in Crankshaft Steels," Proceedings Institution of Mech.
Engrs., Vol. 123, pp. 479-510 (1932).

(30) R. Becker and M. Kornetzki, "Torsional Magneto-Elastic Effects," Zeits. f. Physik,
88, 9-10, pp. 634-644, May 2, 1934.

(31) M. Kersten, "Mechanical Damping of Ferromagnetic Materials by Magnetisation,"
Zeits. f. Tech. Physik, 15, 11, pp. 463-467 (1934).

(32) E. R. Parker, "The Influence of Magnetic Fields on Damping Capacity," Transactions
Am. Soc. Metals, Vol. 28, No. 3, pp. 661-670 (1940).

(33) A. W. Cochardt, "The Origin of Damping in High-Strength Ferromagnetic Alloys,"
Journal of Applied Mechanics, Vol. 20, No. 2, pp. 196-200 (1953).

(34) P. Ludwik, "Bruchgefahr und Materialpruefung," Schweizerischer Verband fuer die Materialpruefung der Technik. Diskussionsber. Nr. 13, Zurich 1928.

(35) P. Ludwik and R. Scheu, "Die Veraenderlichkeit der Werkstoffdaempfung," Zeits. des Vereins Deutscher Ingenieure, Vol. 76, pp. 683-685 (1922).

(36) T. A. Read, "Internal Friction of Single Crystals of Copper and Zinc," Trans. A.I.M.E., Vol. 143, pp. 30-41 (1941).

(37) R. M. Brick and A. Phillips, "Fatigue and Damping Studies of Aircraft Sheet Materials: Duralumin Alloy 24ST, Alclad 24ST, and Several 18-8 Type Stainless Steels," Transactions Am. Soc. Metals, Vol. 29, No. 2, pp. 435-469 (1941).

(38) L. A. Glikman and M. I. Grinberg. Zhur. Tekhn. Fiziki, Vol. 16, p. 985, 1946; Engineers' Digest, Vol. 8, p. 266, 1946.

(39) G. B. Wilkes, Jr., "Changes in Internal Damping of Gas Turbine Materials Due to Continuous Vibration," Transactions Am. Soc. Mech. Engrs., Vol. 71, pp. 631-634, (1949).

(40) R. F. Hanstock, "The Effect of Vibration on a Precipitation-Hardening Aluminium Alloy," Journal Institute of Metals, Vol. 74, Part 9, pp. 469-492 (1948).

(41) G. R. Brophy, "Damping Capacity, a Factor in Fatigue," Transactions Am. Soc. Metals, March, 1936, p. 154.

(42) J. H. Smith, "Some Experiments on Fatigue of Metals," Journal Iron and Steel Inst. (1910) II.

(43) H. J. Gough, "The Fatigue of Metals," D. Van Nostrand, New York, N. Y., p. 244, 1926.

(44) E. Kaufmann, "Ueber die Dauerfestigkeit einiger Eisenwerkstoffe und ihre Beeinflussung durch Temperatur und Kerbwirkung," Berlin 1931, VDI-Verlag.

(45) W. Mason, "Report on Alternating Stress," Rep. Brit. Assoc. (Complex Stress Distribution Ctee.) 1913, p. 183.

(46) B. J. Lazan, "A Study With New Equipment of the Effects of Fatigue Stress on Damping Capacity and Elasticity of Mild Steel," Transactions, Am. Soc. Metals, Vol. 4, pp. 499-558 (1950).

(47) B. J. Lazan and T. Wu, "Damping, Fatigue, and Dynamic Stress-Strain Properties of Mild Steel," Proceedings, Am. Soc. Testing Matr., Vol. 51, pp. 649-681 (1951).

(48) B. J. Lazan and L. J. Demer, "Damping, Elasticity, and Fatigue Properties of Temperature-Resistant Materials," Proceedings, Am. Soc. Testing Mats., Vol. 51, pp. 611-648 (1951).

(49) L. J. Demer and B. J. Lazan, "Damping, Elasticity, and Fatigue Properties of Unnotched and Notched N-155 at Room and Elevated Temperatures," WADC Tech. Rep. 53-70, February 1953.

(50) L. J. Demer and B. J. Lazan, "Damping, Elasticity, and Fatigue Properties of Unnotched and Notched N-155 at Room and Elevated Temperatures," Presented at the 56th Annual Meeting of the Am. Soc. Testing Mats., June 28 - July 3, 1953, Atlantic City, N.J.

(51) NACA Subcommittee on Heat-Resisting materials, NACA Headquarters, "Cooperative Investigation of Relationship Between Static and Fatigue Properties of Heat-Resistant Alloys at Elevated Temperatures," NACA RM 51A04, March 7, 1951.

(52) F. Vitovec and B. J. Lazan, Status Report 53-2 on "Properties of Materials and Joints Under Alternating Force," performed on U. S. Air Force contracts AF-33 (038) 20840, Appendix 32a titled "Fatigue Strength, Damping, and Elasticity Properties of 24S-T4 Aluminum Alloy Under Uniformly Increasing Reversed Stress," 1 April 1953.

(53) F. Vitovec and B. J. Lazan, Status Report 53-3 on "Properties of Materials and Joints Under Alternating Force," performed on U.S. Air Force contracts AF-33 (038) 20840, Appendix 32e titled, "Fatigue, Damping and Elasticity Properties of SAE 1020 Steel Under Uniformly Increasing Reversed Bending Stress," 1 June 1953.

APPENDIX A

DETAILS OF SPECIMEN PREPARATION

Specimens: 24S-T4 Aluminum, J-1 Magnesium, 1020 Steel, and Gray Iron.

Prepared by: John Stulen Co., Gibsonia, Pa.

Procedure:

1. Turning
   Roughed to 0.050 in. oversize.
   Light cut to 0.015-0.020 in. over, feed 0.003 in. per rev.

2. Grinding
   Rough ground to 0.003-0.004 in. oversize in 1 pass.
   Finish ground to 0.002 in. over in 1 pass, longitudinal feed 0.0015 in. per rev.
   Wheels: 4 in. - G.A. 120-06-V10 Aloxite, 3/8 in. wide.
   Coolant: Tycol-Afton 8.

3. Polishing
   Performed by flexible belt on oscillating arm traversing test section during slow or fast rotation of specimen to produce scratches in specimen running in directions of 45 or 135 deg. to longitudinal axis, or approximately parallel to it depending on specimen speed.
   Belts used were grit 180, 400, 600, and 700 (if necessary). At each step fast and slow specimen speeds were used to eliminate the marks from previous step. Final scratch directions were parallel to longitudinal axis.
   Regular carborundum and special belts prepared by Stulen were used.

Specimens: N-155, heat resistant alloy.

Prepared by: Metal Processing Department of the University of Michigan, Ann Arbor, Mich.

Procedure: Description of preparation may be found in NACA RM 51A04 (49).

Specimens: Sandvik Steel, in both conditions of heat treatment.

Prepared by: Sandviken Jernverks, Aktiebolag (turning and grinding) and the Department of Mechanics and Materials, University of Minnesota, Minneapolis, Minn.

Procedure:

1. Turning
   Roughed to 15 mm. diameter on test section using carbide tipped tool. Depth of cut 2 mm. Feed, 0.13 mm. per revolution.
   Finish turning to size including allowance for grinding using high speed steel tool with 0.2 mm. cut. Feed 0.2 mm. per rev.

2. Grinding
    Taper ground to 9.34 - 9.74 mm. on test section with feed of 0.13 mm.
    per revolution.

3. Polishing
    Performed by controlled-pressure belt polishing machine; for details
    see Lazan and Wu (47).
    Rough polishing done with 240 grit belt with kerosene lubricant.
    Finish polish done with 400 grit hair, same lubricant, approximately
    0.0015 in. removed on diameter in each grinding step.

APPENDIX B

DAMPING AND ELASTICITY EQUATIONS FOR INTERPRETING THE ROTATING CANTILEVER BEAM TEST

B. 1 Definition of Symbols and Terms

B = a constant in rotating beam damping equation.

C_m = microscope constant, in. / div.

C, C_1, C_2, C_3 = constants in rotating beam elasticity equations.

D = specific damping energy associated with a given unit stress, in-lb per cu in. per cycle. This, the most basic unit for specifying damping energy, is the energy absorbed per cubic inch of material under conditions of uniform stress.

D_a = average damping energy absorbed per unit volume of stressed material per cycle in-lb per cu in. per cycle; $D_a = D_o/V$. This is not a basic damping unit since, for a given maximum D, the value of D_a depends on the stress distribution. For example, the same material under the same maximum stress (same D) would display a higher D_a under rotating bending than under reverse bending in one plane. Note: D was the symbol used for the average damping in some previous publications (46), (47), (48).

D_o = total damping energy absorbed by specimen per cycle, in-lb / cycle.

D_{of} = total damping energy dissipated in fillets, in-lb / cycle.

D_{ot} = total damping energy dissipated in tapered portion of specimen.

d_t = distance from center of specimen to target, in..

E = modulus of elasticity, tension or compression, psi.

E_{st} = static tangent modulus of elasticity, psi.

E_d = specific dynamic secant modulus of elasticity psi; the value associated with a specific stress or that under uniform stress conditions.

E_{da} = average dynamic secant modulus of elasticity, psi; this is the average or effective value for the specimen in which all stresses from zero to maximum may be present. Note: E_d was the symbol used for the average dynamic modulus in some previous publications (46), (47), (48).

$G = H_o/H = U_o/U$ = ratio of motion at center of gravity of extension arm and its weight, to the motion of the measuring target.

29

H_O = total horizontal traverse (upon reversal of direction of rotation of extension arm) at the center of gravity of loading arm and weight P_O, in.

H = total horizontal reversal at measuring target, in.

H_t = total horizontal reversal at measuring target, microscope divisions.

J = constant in damping-stress equation; the damping energy at a stress of 1 psi.

L = total effective length of specimen, in., $L = L_t + L_f$.

L_f = gage-length equivalent of the two specimen fillets, in.

L_t = gage-length, or length of straight tapered portion of specimen, in.

n = constant in the damping-stress equation; the slope of D_O vs. S_O relationship, at a given stress, on log-log plot.

P = total actual weight of extension arm assembly, lb.

P_e = total effective weight of extension arm assembly, lb.

R = radius of outside fibers of specimen at test section, in.

R_f = ratio of test stress to fatigue strength at 2×10^7 cycles

ρ = radial distance from axis of specimen, in.

S = unit normal fiber stress at any point in specimen, psi.

S_O = maximum unit normal stress at outside fibers of test section of specimen, psi.

U_e = "vertical" deflection at center of gravity of weight P, in. Note: In the case of the tilting table machine, this deflection is measured in the vertical plane but in a direction perpendicular to the table.

U = "vertical" deflection at measuring target, in.

V_e = total effective volume of specimen contributing to the dissipation of of the energy D_O, cu in.

θ = angle between loading arm axis and vertical direction, deg.

θ_ℓ = loading angle for low stress dynamic deflection test, deg.

θ_{test} = loading angle for regular fatigue test, deg.

α = angle between axis of tilting table and vertical direction, deg.

γ = angle between loading arm axis and tilting table, deg. Note: $\gamma = \theta - \alpha$

B. 2 Equations for Converting Experimental Data to Total Specimen Damping, D_o

The outer regions of the rotating cantilever beam specimen are subjected to reversed cyclic stress; tension on the top surface, zero stress at the horizontal position, and compression at the bottom surface. Referring to Fig. 10, a given point on the outer surface of the specimen will traverse circuit D-K-A-B-L-C-D during rotation; stress A is imposed when the point is at the top position and stress C when the point reaches the bottom position. At positions D and B the surface has a definite strain although subjected to zero stress, whereas at points K and L the surface material has zero strain although subjected to a definite stress. The presence of a hysteresis loop, which apparently exists in all materials even at very low stresses, therefore results in an angular shift between the axis of zero bending stress and the axis of zero bending strain. This shift is the cause of the horizontal traversal illustrated in Fig. 11.

Explaining further the reason for the horizontal traversal, one might consider the fibers at A in a position of maximum tensile stress and strain and those at C in a similar position for compression. After 90° of rotation from this position the fibers which are at A are then at zero stress but are elongated over their unstressed length by the strain OB. The fibers which were at C then have zero stress, but residual compressive strain and are shortened over their unstressed length by strain OD. The lengthening of the fibers on one side of the specimen and shortening of those on the other side are responsible for the lateral displacement of the end of the rotating cantilever beam. On reversal of direction of rotation of the specimen, the lateral displacement is in the opposite direction. The sum of the two displacements is the horizontal traversal illustrated in Fig. 11.

That a horizontal traversal must exist and is associated with hysteresis damping is also apparent from still another point of view. The presence of a hysteresis loop indicates that the specimen is absorbing energy proportional to the area within the hysteresis loop. This energy absorption can be associated with a resisting torque which requires a horizontal traversal of the loading weight in that direction which will always create a resisting torque on the system (to right for counterclockwise rotation facing the target as shown in Fig. 11 and to the left for clockwise rotation). Thus, the total energy absorbed by the specimen in in.-lb per cycle due to damping within the specimen is:

$$D_o = 2\pi(\text{resisting torque})$$

$$= 2\pi P_o \, H_o/2$$

$$= \pi P_o \, H_o \tag{B-1}$$

In terms of displacements at the target instead of at the center of gravity of the loading arm, the above equation becomes:

$$D_o = \pi G \, P_o \, H \tag{B-2}$$

The ratio, G, depends on the position of the effective center of rotation of the extension arm during specimen deflection. The location of this point was found to be very close to the center of the specimen (longitudinally) particularly since the ratio of specimen length to extension arm length is small. Therefore, the center of rotation of the extension arm is assumed to be at the center of the specimen for reasons of simplicity, an assumption which involves an error of less than 1 percent.

Equation B-2 applies to the horizontal rotating spindle assembly shown in Fig. 11, in which P_0 is the effective weight of the loading arm assembly. For the tilting table machine also shown in Fig. 11, the effective moment producing weight is:

$$P_0 = P \sin \theta.$$

Thus for the tilting table machine, the expression for D_0 becomes:

$$D_0 = \pi G P H \sin \theta \qquad (B-3)$$

Since the maximum cyclic stress, S_0, in the specimen is proportional to $P \sin \theta$, the total damping capacity is proportional to $S_0 H$. Therefore, for a given specimen shape, Eq. A-3 may be rewritten:

$$D_0 = \text{constant } S_0 H \qquad (B-4)$$

with the constant being dependent only on the specimen shape and the type of machine used in the tests.

For the actual tests run in the laboratory, the table angle, α, is read from a scale attached to the machine. The correction angle, γ, which accounts for the increase in angle of the loading arm due to the specimen deflection, may be obtained from:

$$\gamma = \text{arc tan } \frac{H}{a_f}$$

If displacement is used in microscope divisions, H_f, then the expression for total damping becomes:

$$D_0 = \pi G P H_f C_m \sin (\alpha + \gamma) \qquad (B-5)$$

and if a constant is chosen having the value:

$$B = \pi G P C_m \sin (\alpha + \gamma)$$

then the expression for total damping during a test at constant stress is:

$$D_0 = B H_f \qquad (B-6)$$

The above expression gives the total damping for the entire specimen (straight tapered section plus fillets). It is desirable, however, to obtain a quantity which is independent of the shape and stress distribution of the specimen. Before deriving an expression by which the total damping, as given by Eq. B-6 may be converted to specific damping D, it is necessary to investigate, first, the relationship between D and D_0 in a specimen without fillets, and secondly, to determine the gage-length equivalent of the fillets for the specimens used in the actual tests. These factors will be taken up in order in the following sections.

B.3 Relationship Between Total Damping Energy and Specific Damping Energy in a Solid Specimen Without Fillets for Case When $D = J S^n$

The relationships obtained below refer to cylindrical specimens under conditions of constant maximum rotating bending stress along the length of the specimen. For the symbols used refer to Fig. 12. The assumption is made in this section that the specific damping energy,

32

D, at a constant stress history and temperature may be represented by the equation:

$$D = J S^n \qquad (B-7)$$

Recent work indicates that the relationship between damping and stress may be more complicated in certain stress ranges and for certain materials than that indicated by Eq. B-7. Therefore, in Section B.5, which follows, a graphical method is presented so that this simplified relationship need not be assumed over the whole stress range. The total damping in the specimen subjected to reversed stress is:

$$D_o = \int D \, dV = \int D \frac{dV}{dS} \, dS \qquad (B-8)$$

For the rotating beam test the volume-stress function, of which dV/dS is the slope, may be determined as indicated below for a solid specimen of length L. With reference to Fig. 12:

$$S = \frac{\rho}{R} S_o \quad \text{and} \quad \rho = \frac{S}{S_o} R$$

Also, if V is taken as that volume having a stress less than S, then:

$$V = \pi \rho^2 L = \pi \frac{S^2}{S_o^2} R^2 L = \frac{V_o}{S_o^2} S^2$$

and

$$\frac{dV}{dS} = 2 \frac{V_o}{S_o^2} S$$

Substitution in Eq. B-8 gives D_o, the total damping energy in the specimen, for a maximum stress equal to S_o:

$$D_o = 2 \frac{V_o}{S_o^2} \int_o^{S_o} D \, S \, dS \qquad (B-9)$$

Substituting the assumed expression B-7 for D in Eq. B-9 gives:

$$D_o = 2 \frac{V_o}{S_o^2} \int_o^{S_o} J \, S^{n+1} \, dS \qquad (B-10)$$

This expression integrated reduces to:

$$D_o = \frac{2 V_o J S_o^n}{n+2} \qquad (B-11)$$

33

If the specific damping is to be determined at a stress equal to S_o, then:

$$D = J S_o^n$$

and Eq. B-11 becomes:

$$D_o = \frac{2 V_o D}{n+2} \tag{B-12}$$

from which,

$$D = \frac{n+2}{2} \frac{D_o}{V_o} \tag{B-13}$$

Assuming a linear relationship between log D and log S, then Eq. B-12 indicates that the total damping energy of the specimen is equal to a constant multiple of the specific damping D for a constant specimen effective volume. Solving for the specific damping, Eq. B-13 provides a method for obtaining the specific damping from the total damping curve provided a linear relationship exists between log D_o and log S_o.

Comparison of Eqs. B-7 and B-11 indicates that the log-log curves for both total and specific damping have the same slope value n.

B. 4 Determination of the Gage-Length Equivalent of the Specimen Fillets

A practical difficulty in the use of Eq. B-13 results from the fact that specimens with fillets are used in the actual tests. The total damping which is measured (and evaluated from Eq. B-6), therefore, is not that due to the straight tapered portion of the test specimen alone, for which the maximum stress at the outer fibers is constant, but includes also the energy dissipated by the fillets on both ends of the specimen. The maximum fiber stress along the fillets decreases rapidly from S_o as the diameter increases. Furthermore, the energy dissipation decreases at an even greater rate since the damping is a power function of the stress. It is necessary, however, to determine a gage-length equivalent, L_f, for the fillets to be added to the length of the straight tapered portion, L_t, of the test specimen in order to determine the effective length, L, which is used in calculating the effective volume, V, for the specimen.

A rigorous analytical determination of the damping energy of the fillets becomes rather involved and the results would be cumbersome to use since the damping energy dissipated by a given element of cross section along the fillet is a function both of the stress distribution along the fillet and also the stress distribution at the section. Furthermore, the variation of damping with stress is not, for all materials, a simple function of the stress. Therefore, an approximation to the gage-length equivalent for the fillets seems best made by a method of solution involving graphical integration. The steps followed in one such method are

1. The fillet volumes are divided into incremental slices perpendicular to the specimen axis and of arbitrary thickness, as shown in Fig. 13.
2. The average maximum stress for each slice in percent of the maximum test stress, S_o, is computed from the section modulus for the diameter at the center of the slice and the loading moment existing at that section.
3. The approximate volume of each slice is computed from the diameter at the center of the slice.

4. In order to determine the energy dissipation in each slice, an assumption is made regarding the variation of damping with stress. In many materials previously investigated, the total damping in the specimen is related to the stress by the general formula, $D_o = J S_o^n$. In some cases, as discussed in the body of this report, one equation satisfies the damping behavior below the cyclic stress sensitivity limit, in which range damping is unaffected by stress history, while above this range the same form of equation is approximately satisfied but usually with different values of J and n for each fixed number of cycles in the stress history. In any event, for an approximate correction for the energy dissipated in the fillets, it would appear reasonable to assume such a variation between the specific damping and the stress as that given above. On the basis of this assumption, the relationship between total damping and the maximum stress in the specimen will also have the same coefficient n. This fact is obvious from Eq. B-12 which shows D_o to be a constant multiple of D.

5. The energy dissipated in the straight tapered portion of the specimen for an assumed S_o may be calculated (employing Eq. B-13) from:

$$D_{ot} = \frac{2}{n+2} D V_t \qquad (B-14)$$

where V_t is the volume of the straight tapered portion of the solid specimen.

6. In a similar manner, the energy dissipated in each slice of fillet for an assumed S_o may be calculated from the volume of the slice and the average maximum stress for the slice in percent of S_o.

7. The sum of the energy lost in all the slices is totaled to give D_{of}, the total energy dissipated in the fillets.

8. The equivalent length of the two fillets in terms of length of the straight tapered portion of the specimen may be calculated from:

$$L_f = \frac{D_{of}}{D_{ot}} L_t \qquad (B-15)$$

The above procedure is carried out for various assumed relationships of D and S, that is, for straight lines of various slopes on a log D vs. log S plot. In this manner sufficient values are obtained to make a plot of the gage-length equivalent of the fillets vs. n for the type E specimen employed in the tests. Such a plot is shown in Fig. 14 for the type E specimen used in this investigation. As observed from this graph, a change in slope from n = 3 to n = 9 results in a change in gage-length equivalent of from 0.34 in. to 0.19 in. This corresponds to a change of from about 19 percent to about 11 percent of the length of the straight tapered portion of a type E specimen.

When performing the actual damping tests, the total damping values as obtained from Eq. B-5 are plotted from experimental data in the form of a D_o-S_o-N diagram (similar to Fig. 3 for Sandvik steel, normalized). If the relationship between total damping and maximum test stress in the specimen is found to be a straight line on the log-log plot of D_o vs. S_o, then the corresponding relationship between specific damping D and unit stress S has the same slope, n. The gage-length equivalent of the fillets may be obtained from the curve for the particular specimen showing L_f vs. log n. The effective volume, V, of the solid specimen is then computed from:

$$V = \frac{\pi D^2}{4} (L_t + L_f) \qquad (B-16)$$

35

If, however, the observed relationship for D_o vs. S_o for the material being studied is a curved line on a log-log plot or is made up of two straight line portions of different slope, then an approximation is necessary to determine the gage-length equivalent by the method discussed above. One way of obtaining an n value with which to make the determination in such a case is by using a secant slope measured from the plot of log D_o vs. log S_o, using some arbitrary point on the log scale as an index for the measurement of the slope value. Obviously this method involves some uncertainty; however, since this is an approximation only in a correction to the original data, it is thought to be sufficiently precise for the purpose.

If the D_o vs. S_o curves for each number of cycles in the stress history of the specimen have different slope values on the log-log plot above the cyclic stress sensitivity limit, then a different gage-length equivalent for the fillets should be applied for each curve and for each stress value on the curve in converting from D_o to D. In practice, however, this need be done only for a few stresses to obtain enough points for sketching in the curve.

B.5 Graphical Method for Determining Specific Damping From Total Damping for Various D_o vs. S_o Relationships

In some cases the log D_o vs. log S_o curve obtained experimentally can be approximated by a straight line throughout the range of stress investigated. In other instances the data satisfy a straight line relationship closely only over a certain stress range. This range usually extends from the lowest stresses investigated up to approximately 70 to 90 percent of the fatigue strength for the material. For some materials, the curve for a given stress history then curves sharply upward and continues in approximately a straight line, but of much higher slope than at the lower stresses. Often, the curve for each number of cycles in the stress history has a different slope. In other instances, materials are encountered for which the curves for log D_o vs. log S_o, above a certain linear range, are curved lines of slowly but continuously increasing slope. In still other cases, for example, materials having high magneto-striction damping, the specific damping vs. stress curves may even display a pronounced plateau beyond a certain stress.

In cases where the log slope n is constant throughout the whole stress range, then specific damping values may be computed from the experimentally obtained total damping values by the use of Eq. B-13. Relationships are required, however, for the conversion of D_o to D in the cases where the log D_o vs. log S_o relationship is approximated by two straight lines of different slope or where the relationship is linear up to a certain value of stress but then has an increasing value of n at the higher stresses. A method for use in such instances is given below.

As previously explained, the total damping in a member subjected to reversed cyclic stress is given by Eq. B-8:

$$D_o = \int D \, dV = \int D \, \frac{dV}{dS} dS$$

For parts like a compressor blade having a complicated stress distribution, the volume-stress function must be determined from design data and loading information or by direct measurements. In these instances, $\frac{dV}{dS}$, in the equation above, may be handled graphically. For the case of the rotating cantilever beam, however, the expression for total damping D_o for a maximum stress equal to S_o was shown by Eq. B-9 to be:

36

$$D_o = \frac{2 V_o}{S_o^2} \int_0^{S_o} D \; S \; dS$$

When D can be expressed as a simple mathematical function of the stress, then no dif-
ficulty is encountered, for straightforward integration is possible. For the cases to be
considered now, however, D can not be expressed as a simple mathematical function
of S and the integral cannot be readily evaluated mathematically. An alternative
graphical procedure is outlined below.

With reference to Fig. 15, D_{o1}, D_{o2}, D_{o3}, ...D_{on}, and D_1,
D_2, D_3, ...D_n, are defined as specific values of total damping energy, D_o, and
specific damping energy, D, respectively, at the specific stresses, S_1, S_2, S_3, ...S_n.
In any D vs. S relationship, log linearity may be assumed up to a certain stress S_1, this
stress being selected low enough to make the error in this assumption insignificant. In this
range the relationship between specific damping and stress is satisfied by:

$$D = J \; S^n$$

The log slope n of the D curve in this range is identical to that for the D_o
curve, and the specific damping values may be computed by the use of Eq. B-13. Be-
yond the stress where the log linearity no longer exists, the data satisfy a different function
for D and application of Eq. B-13 is no longer valid.

For conversion of the D_o data to D values beyond the linear range, consider
the following. Using the notation in Fig. 15 and applying Eq. B-9:

$$D_{o1} = \frac{2 V_o}{S_1^2} \int_0^{S_1} {}_oD_1 \; S \; dS \tag{B-17}$$

$$D_{o2} = \frac{2 V_o}{S_2^2} \left[\int_0^{S_1} {}_oD_1 \; S \; dS + \int_{S_1}^{S_2} {}_1D_2 \; S \; dS \right] \tag{B-18}$$

In the above equations ${}_oD_1$ is used to designate a function of stress for $s \leq s_1$, and ${}_1D_2$
is used to designate a different function of stress for $s_1 \leq s \leq s_2$. Then upon substituting
the value of the integral from Eq. B-17 into Eq. B-18 there results the relationship.

$$D_{o2} = \frac{S_1^2}{S_2^2} D_{o1} + \frac{2 V_o}{S_2^2} \int_{S_1}^{S_2} {}_1D_2 \; S \; dS \tag{B-19}$$

In a graphical integration in which the integration slices are small enough to
assume without significant error that, over a small increment in stress, D has a straight line
relationship with S on a linear plot, then the integral of Eq. B-19 may be reduced as shown
below. For the discussion, refer to Fig. 15.

37

$$\int_{S_1}^{S_2} {}_1 D_2\, S\, dS = \text{moment of area under D-S diagram between } S_1 \text{ and } S_2 \text{ about stress origin.}$$

$$= \left(\frac{D_1 + D_2}{2} \right) \Delta S \left(\frac{S_1 + S_2}{2} \right)$$

Solving for D_2 from Eq. B-19, the above expression given:

$$D_2 = \frac{2 \left(D_{o2}\, S_2^2 - D_{o1}\, S_1^2 \right)}{V_c \Delta S \;(S_1 + S_2)} - D_1 \tag{B-20}$$

This equation then may be used to determine the values for D_2 in the stress range beyond the region of logarithmic linearity as illustrated in Fig. 15. The smaller the interval ΔS the more accurate is Eq. B-20. Having found D_2, it is then possible to determine D_3 by the same equation, then D_4, etc., as indicated by the general equation shown for Range 3 in Fig. 15. This stepwise process may be checked periodically by graphically integrating the D curve as indicated by Eq. B-9.

B. 6 Determination of Average Dynamic Modulus of Elasticity From Vertical Deflection Measurements in the Rotating Cantilever Beam Test

The modulus of elasticity, E, of the test specimen material is directly proportional to the ratio of the effective moment producing load, $P \sin \theta$, to the vertical deflection, U, as defined previously. Thus:

$$E = C \frac{P \sin \theta}{U} \tag{B-21}$$

The constant, C, depends on the effective specimen length, the moment of inertia along its length, and the location of the center of gravity of the loading weight, P. Since the specimen stress is proportional to $P \sin \theta$, the modulus may also be expressed as:

$$E = C_1 \frac{S}{U} \tag{B-22}$$

If U is measured on a non-rotating beam, then E is the static modulus of elasticity, E_{st}, whereas if the beam is rotating and receiving cyclic stress, then the modulus of elasticity calculated from U is the dynamic value E_{da}.

The constant C may be determined by three different methods: (a) calculation of the elastic deflection curve by the double integration method, (b) calculation of the maximum deflection by a graphical moment-area method, and (c) experimental determination of the constant for each specimen prior to the start of an actual test. Of these, the experimental method proves to be the most useful.

The double integration method becomes rather tedious and complex for certain shapes of specimens. It proves to be too lengthy for practical use in most cases.

The graphical moment-area method is discussed in detail in the Appendix to reference (44). In using the equations associated with this method, it is necessary that extremely accurate measurements be made of specimen dimensions, since the constant C is critically dependent on the specimen length and diameters.

It is more accurate, therefore, for most types of specimens to determine the constant C, which is essentially a specimen stiffness constant, by experimental methods. Two such methods have been successfully used: (a) determination of the natural frequency of vibration of the specimen-extension arm system during a low stress vibration decay test prior to starting the cyclic stress test and (b) determination of the deflection curves for small stresses before the cyclic stress test is started.

The deflection method is favored over the vibration method because of ease of application and reliability of results. For a determination of the specimen constant by this method, a damping-fatigue specimen is set up in the testing machine in the usual manner for a dynamic test. Before the actual test is started, however, readings of vertical deflection at the target are made for various angle settings up to stresses of about 50 percent of the expected fatigue limit of the material. These tests may be performed on a non-rotating specimen or on a rotating specimen, for in the materials investigated there is no detectable difference between the static and dynamic moduli in the low stress range. It is preferred to have the specimen rotating slowly, however, for this prevents permanent set (especially in the small diameter specimens) which introduces run-out in the subsequent dynamic test.

When the vertical target deflection readings are plotted as a function of the sine of the table angle, the points fall on a straight line. It is, therefore, relatively easy to establish a curve with a small number of points. At a convenient value of the sine, the deflection is read from the curve. Two corrections should be applied to this set of readings. The correction angle should be added to the table angle a to give true loading angle θ, as discussed in the section dealing with damping. The second correction is required because of the fact that the deflection as measured includes not only that due to bending in the specimen but also that due to elasticity in the joints, in the extension arm, and in the tilting table itself. The so-called "calibration correction" for these latter factors is determined prior to specimen testing by making deflection tests on a given machine with a dummy specimen mounted in position. The deflection due to the joints, arm, and table may be isolated by subtracting from these deflection readings a calculated deflection at the target due to bending in the dummy specimen. Thus, after correcting the angle and correcting the observed low stress deflection readings, a constant, proportional to a specimen shape constant, may be obtained from:

$$C_2 = \frac{E_{st} U_\ell}{\sin \theta_\ell} \qquad (B-23)$$

The subscripts are intended to indicate the corrected values obtained from the low stress deflection test made on the actual test specimen.

The corrections discussed above are applied to observations made during the actual fatigue test at a given table angle to obtain $\sin \theta_{test}$ and a corrected U_{test}. The average dynamic modulus of elasticity may then be determined from each observation of vertical target position by substitution in:

$$E_{da} = C_2 \frac{\sin \theta_{test}}{U_{test}} \qquad (B-24)$$

$$E_{do} = \left(E_{st} \frac{U_\phi \sin \theta_{test}}{\sin \theta_\phi} \right) \frac{1}{U_{test}} \tag{B-25}$$

$$E_{do} = \frac{C_3}{U_{test}} \tag{B-26}$$

Since the changes in deflection ordinarily encountered during the course of a test at a given table angle are, in general, insufficient to cause an appreciable change in θ_{test}, all of the factors grouped in brackets above may be combined into a constant C_3, so that a simple division suffices to convert from the vertical deflection measured at a given number of cycles to the corresponding dynamic modulus of elasticity value.

It should be pointed out that the dynamic moduli values obtained are secant values since they are determined from maximum strain readings such as those corresponding to point A in Fig. 10.

TABLE I -- CHEMICAL COMPOSITION, PRODUCTION, AND TREATMENT

Name of Material	Source	Chemical Composition, per cent	Production and Heat Treatment
Sandvik Steel (N)	Sandvikens Jarn-verks Aktiebolag Sandviken, Sweden	1.02Cr, 0.98C, 0.26Mn, 0.24Mo, 0.22Si, 0.014S, 0.028P, 0.02Cu, 0.01Ni, (bal) Fe	Hot rolled bar stock, 1 in. hex of acid open hearth steel. Normalized by resistance heating to 1905 F. Cooled in still air.
Sandvik Steel (Q-T)	Sandvikens Jarn-verks Aktiebolag Sandviken, Sweden	1.02Cr, 0.98C, 0.26Mn, 0.24Mo, 0.22Si, 0.014S, 0.028P, 0.02Cu, 0.01Ni, (bal) Fe	Hot rolled bar stock, 1 in. hex, of acid open hearth steel. Heated to 1905 F, quenched in oil at 1515 F (15 minutes at heat). Drawn at 1095 F for 1 hour.
1020 Steel	Crucible Steel Co., Syracuse, New York	0.3 to 0.6Mn, 0.15 to 0.25C, 0.055 (max) S, 0.45 (max) P, (bal) Fe	Hot rolled bar stock 1-5/8 in. diameter of electric melted steel, specially controlled for uniformity and cleanliness.
N-155 Alloy	Universal-Cyclops Steel Corp., Bridleville, Pa.	21.7Cr, 19.4Ni, 19.0Co, 2.76Mo, 1.90W, 1.74Mn, 0.76Cb, 0.37Si, 0.15C 0.14N, 32.1 (bal) Fe	15.5 ingot hammer cogged to 2in square. Rolled to 1 in. rounds at 2050-1830 F. Water quenched from 2200 F. Aging treatment - 1400 F for 16 hrs., air cooled
Gray Iron	Straight Line Foundry & Machine Company Syracuse, N.Y.	3.65C, 2.46Si, 0.73Mn, 0.265P, 0.132S, 92.75 (bal) Fe	1-1/4 in. x 20 in. regular arbitration bars as cast.
24S-T4 Aluminum	Aluminum Corporation of America, New Kensington, Pennsylvania	4.20Cu, 1.46Mg, 0.63Mn, 0.30Fe, 0.14Si, 0.07Zn, 0.02Cr, 0.02Ti, (bal) Al	Rolled bars 1-1/8 in. diameter, solution heat treated at 915 F.
J-1 Magnesium	Dow Chemical Company, Midland, Michigan	7.2 to 5.8Al, 0.4 to 1.5Zn, 0.3 (max) Si, 0.15 (min) Mn, 0.05 (max) Cu, 0.005 (max) Fe, (bal) Mg	Extruded bars 1-5/8 in. diameter, used in this condition.

TABLE II — SUMMARY OF EXPERIMENTAL RESULTS

Property	Sandwich Steel (9-1)	Sandwich Steel (9)	N-155	SAE ?	2024-? Al	?-? Mg	? Gray Iron
STATIC							
Yield Strength, 0.2% offset, psi	177 000	116 000	40 800	46 000	46 000	33 000	
Tensile Strength, psi	209 700	186 700	119 000	71 300	72 000	40 000	29 000
Elongation in 2 in., %		4.1	43.7	25.0	21.4	14.8	
Reduction of Area, %	21	11	46	60.5			
Modulus of Elasticity, 10^6 psi	25.5	29.2	30.0	59.4	10.6	6.0	22.0
FATIGUE							
Fatigue Strength at 2 x 10^7 cycles, psi	92 000	76 000	53 000	35 000	27 000	17 000	? 000
Ratio of FS to Static Tensile Strength	0.45	0.41	0.445	0.50	0.37	0.37	0.47
DAMPING							
Approx. Stress at Cyclic Strain Sensitivity Limit, psi	100 000	55 000	33 000	30 000	24 000	8 000	4 200
Ratio of Stress at CSSL to FS at 2 x 10^7 cycles	1.1	0.7	0.6	0.85	0.9	0.5	0.7
Ratio of Stress at CSSL to Static TS	0.5	0.3	0.3	0.4	0.3	0.2	0.3
Specific Damping Energy at CSSL, in-lb per cu in. per cycle	2.5	1.3	0.4	0.45	0.45	0.1	0.7
Slope of log D vs. log S line below CSSL	2.1	2.4	2.5	2.0	2.0	2.0	2.4
Slope Range of log D vs. log S line above CSSL	3.5-17	10-12	7-10	10-21	3-14	2-7	2-3
Specific Damping Range at FS at 2 x 10^7 cycles, in-lb per cu in. per cycle	2.3	10-70	24-48	0.7-25	0.4-10	0.5-1.2	1.2-1.7
ELASTICITY							
Approx. Dynamic Proportional Limit, psi	100 000	50 000	40 000	30 000	36 000	14 000	
Ratio of DPL to FS at 2 x 10^7 cycles	1.1	0.65	0.75	0.85	1.3	0.8	
Ratio of DPL to Stress at Damping CSSL	1.0	0.9	1.2	1.0	1.5	1.75	
Ratio of DPL to Static TS	0.5	0.3	0.35	0.4	0.5	0.3	
Average Dynamic Modulus at FS as per cent of Static Modulus	100	95-99	97-98	97-99.5	100	100	90-?
Approx. Strain at FS, in. per in.	0.00014	0.00270	0.00180	0.00125	0.00235	0.00261	0.00245
Approx. Strain at Damping CSSL, in. per in.	0.00041	0.00190	0.00108	0.00105	0.00224	0.00130	0.00041
DAMPING ENERGY COMPARISONS							
Damping Energy at Stress of 6000 psi	0.0045	0.0020	0.006	0.015	0.036	0.063	0.05
Damping Energy at a Ratio of Stress to Fatigue Strength at 2 x 10^7 cycles Equal to 0.4	0.27	0.27	0.15	0.10	0.09	0.046	0.125
Damping Energy at Strain Equal to 0.0004 in. per in., in-lb per cu in. per cycle	0.032	0.022	0.025	0.079	0.014	0.01	0.05
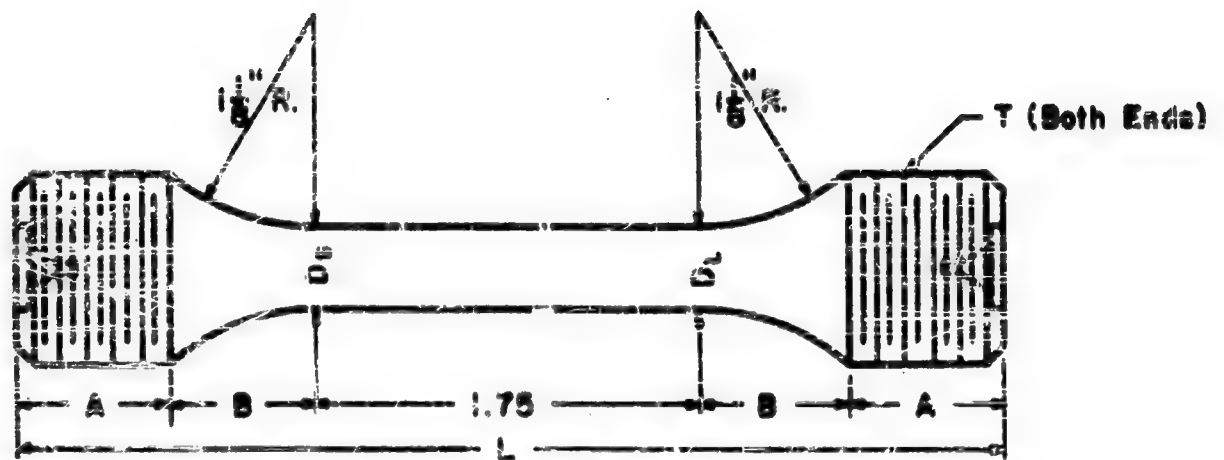
Specimen Designation	A(in)	B(in)	D_S(in)	D_L(in)	L(in)	T(in)
C	1	$\frac{5}{8}$	.5754	.5960	$4\frac{1}{2}$	$\frac{7}{8}$ 14NF
D	$\frac{7}{8}$	$\frac{3}{4}$	.5754	.5960	$4\frac{1}{2}$	$1\frac{1}{8}$ 12NF
E	$\frac{1}{2}$	$\frac{3}{8}$	.2018	.2100	4	$\frac{5}{8}$ 18NF
L	$\frac{11}{16}$	$\frac{11}{16}$	.3677	.3820	$4\frac{1}{2}$	$\frac{7}{8}$ 9NF

Fig. 1 — Rotating Beam Damping, Elasticity, and Fatigue Test Specimens.
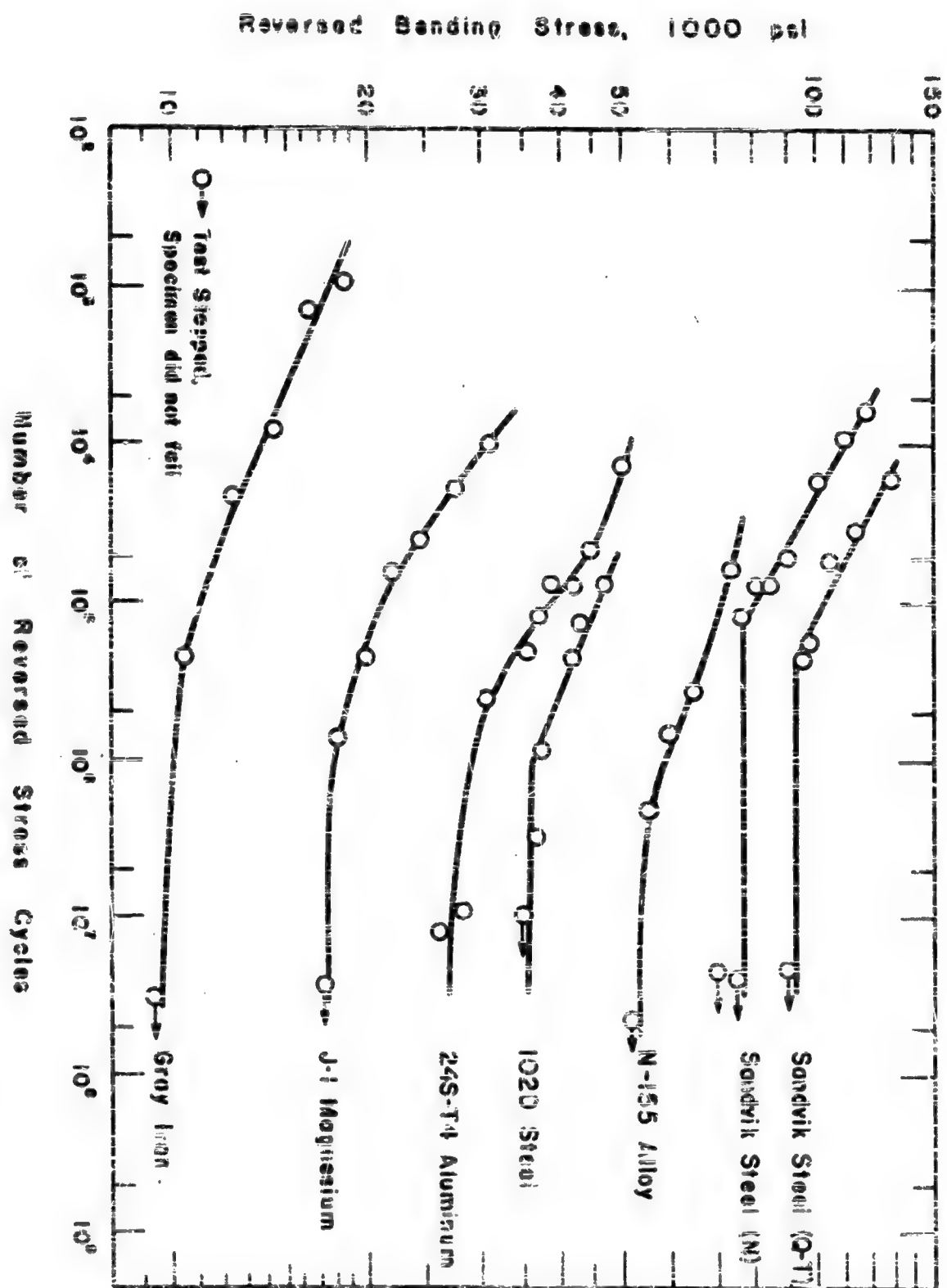
Fig. 2.— S-N Fatigue Curves of Stress Versus Cycles to Fracture for Unnotched Specimens of Various Materials.
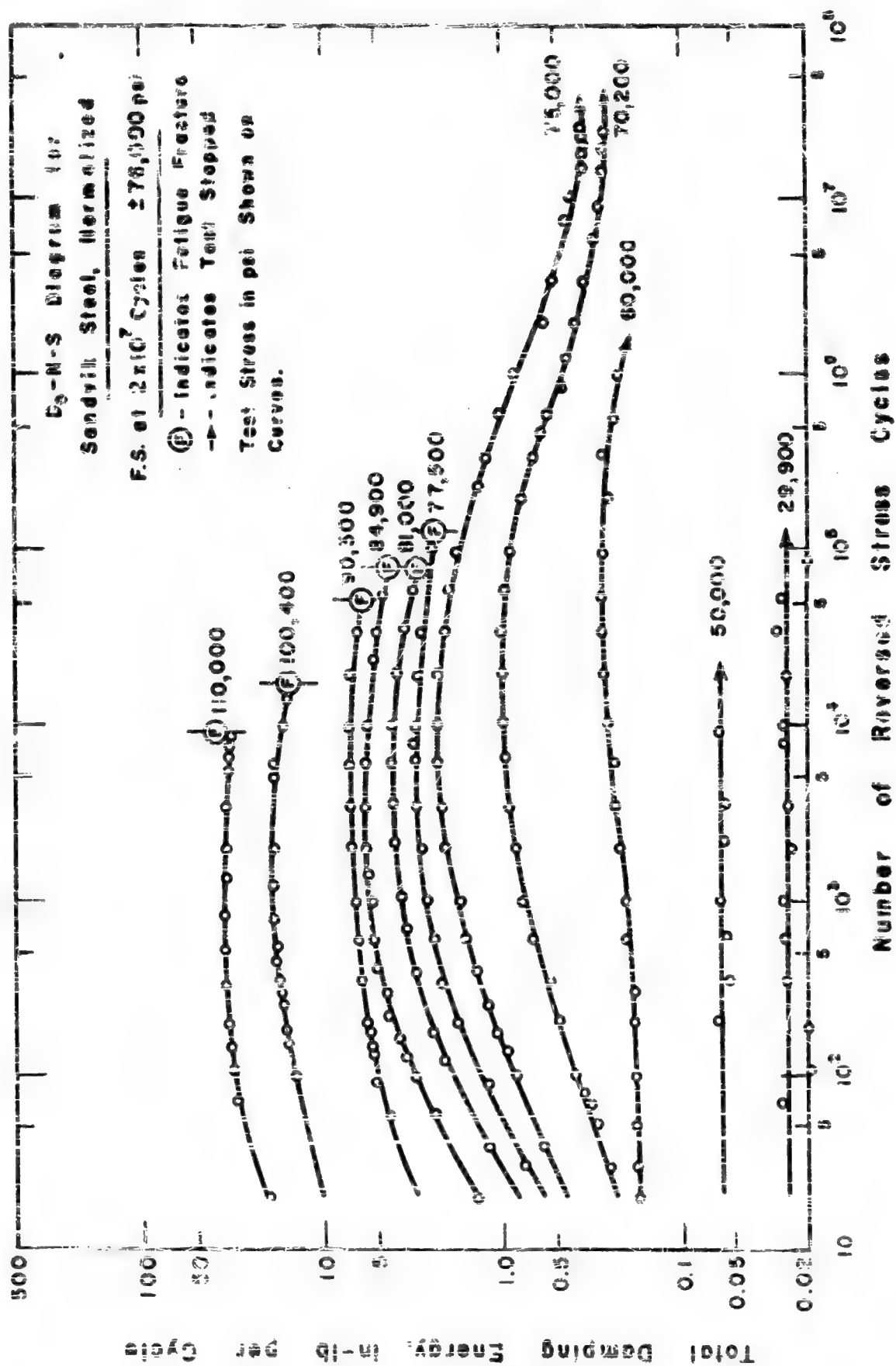
Fig. 3 — Effect of Sustained Cyclic Stress of Several Magnitudes on Damping Energy of Unnotched Specimens of Sandvik Steel Normalized.
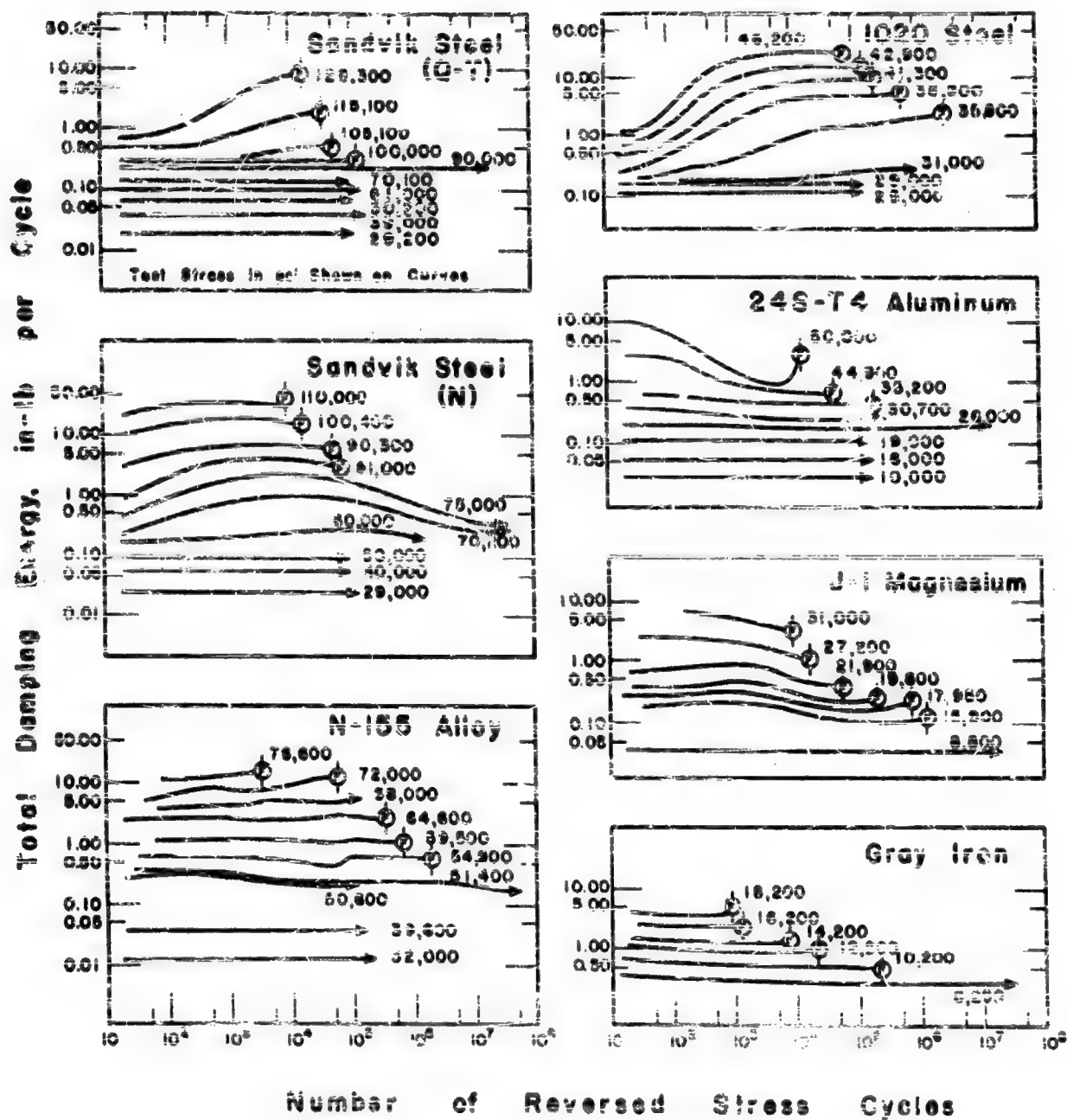
Fig. 4 - Comparison of the Effect of Sustained Cyclic Stress of Several Magnitudes on the Unnotched Damping Energy of Various Materials.
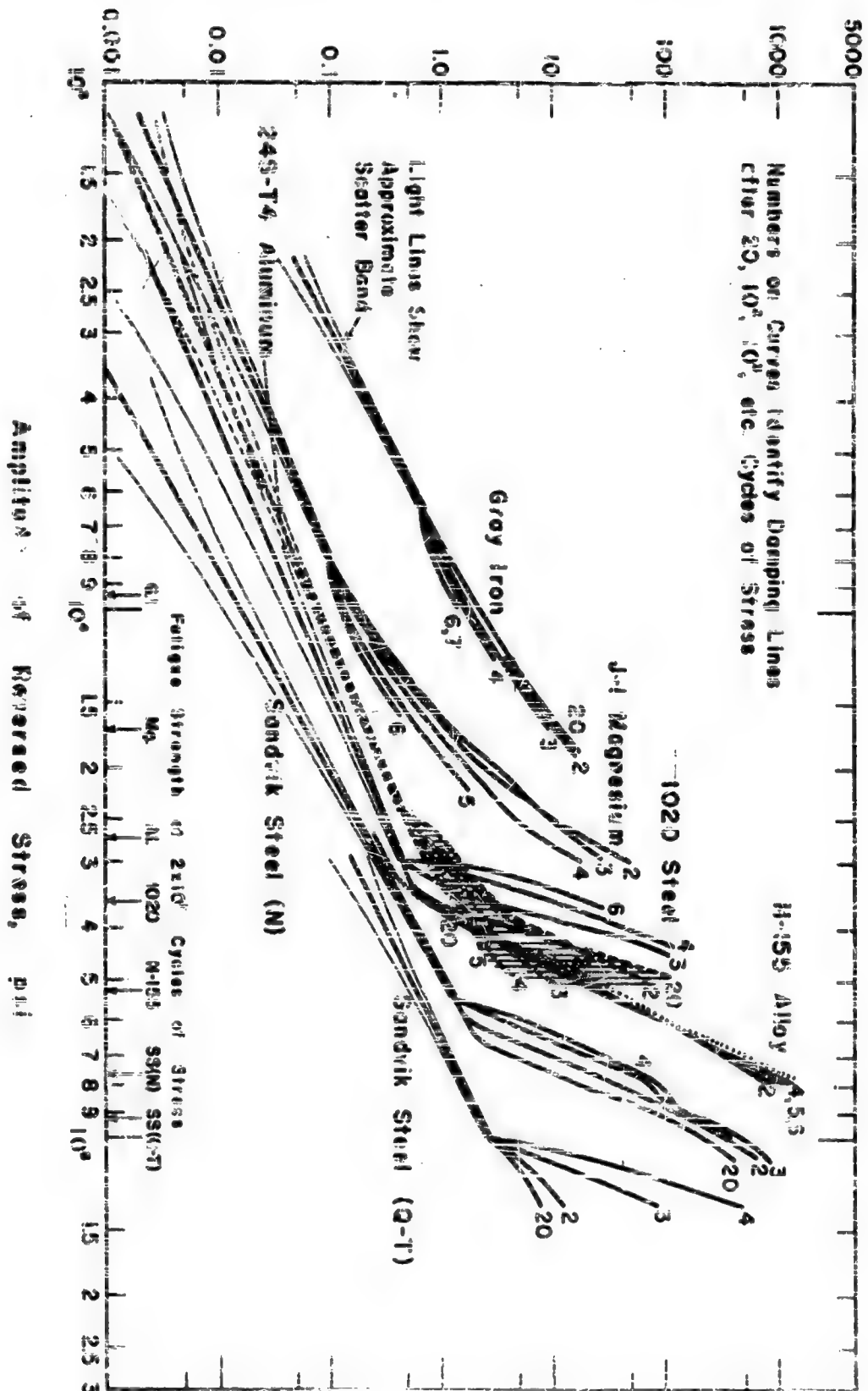
Fig. 7 — Specific Damping Energy of Various Materials as a Function of Amplitude of Reversed Stress.
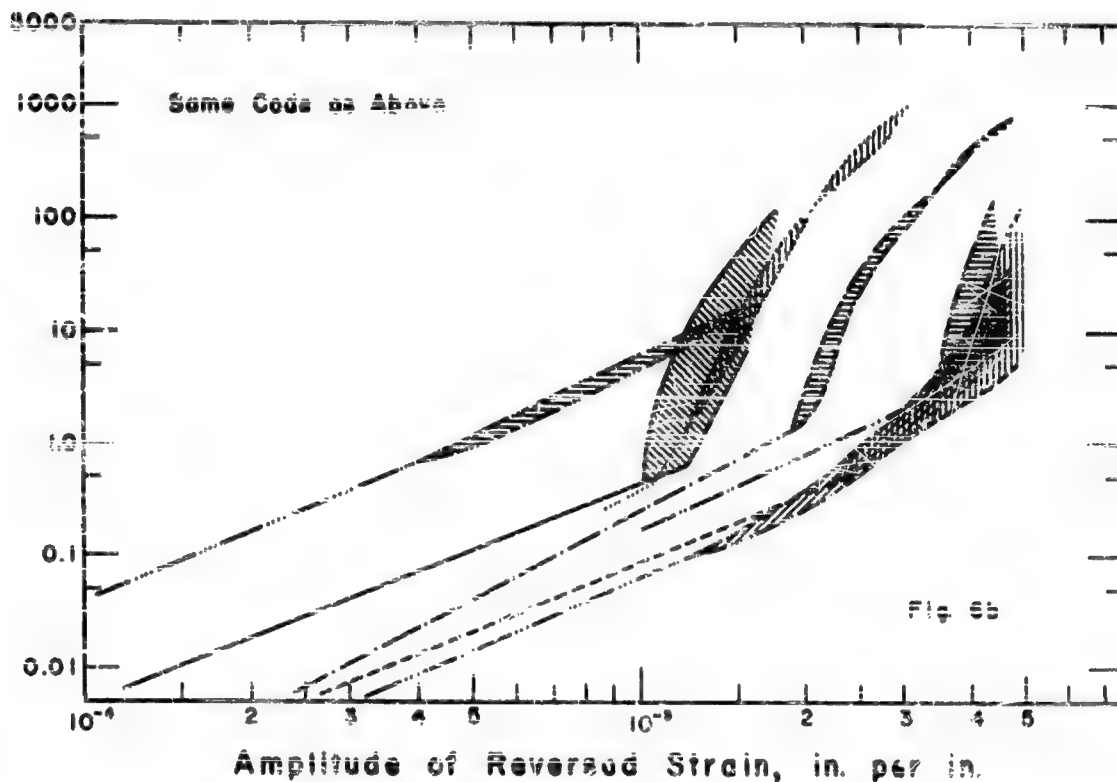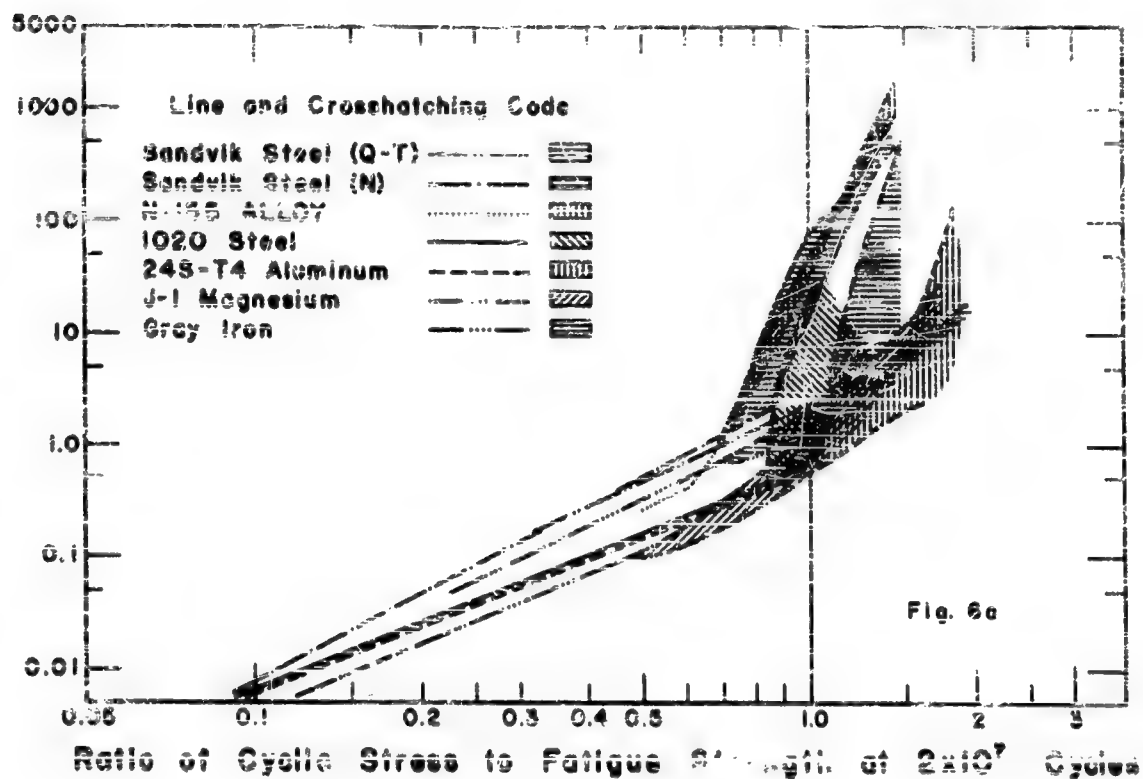
Fig. 6 – Specific Damping Energy of Various Materials Shown Both as a Function of Stress Ratio and Strain Amplitude at Outer Fibers.

48
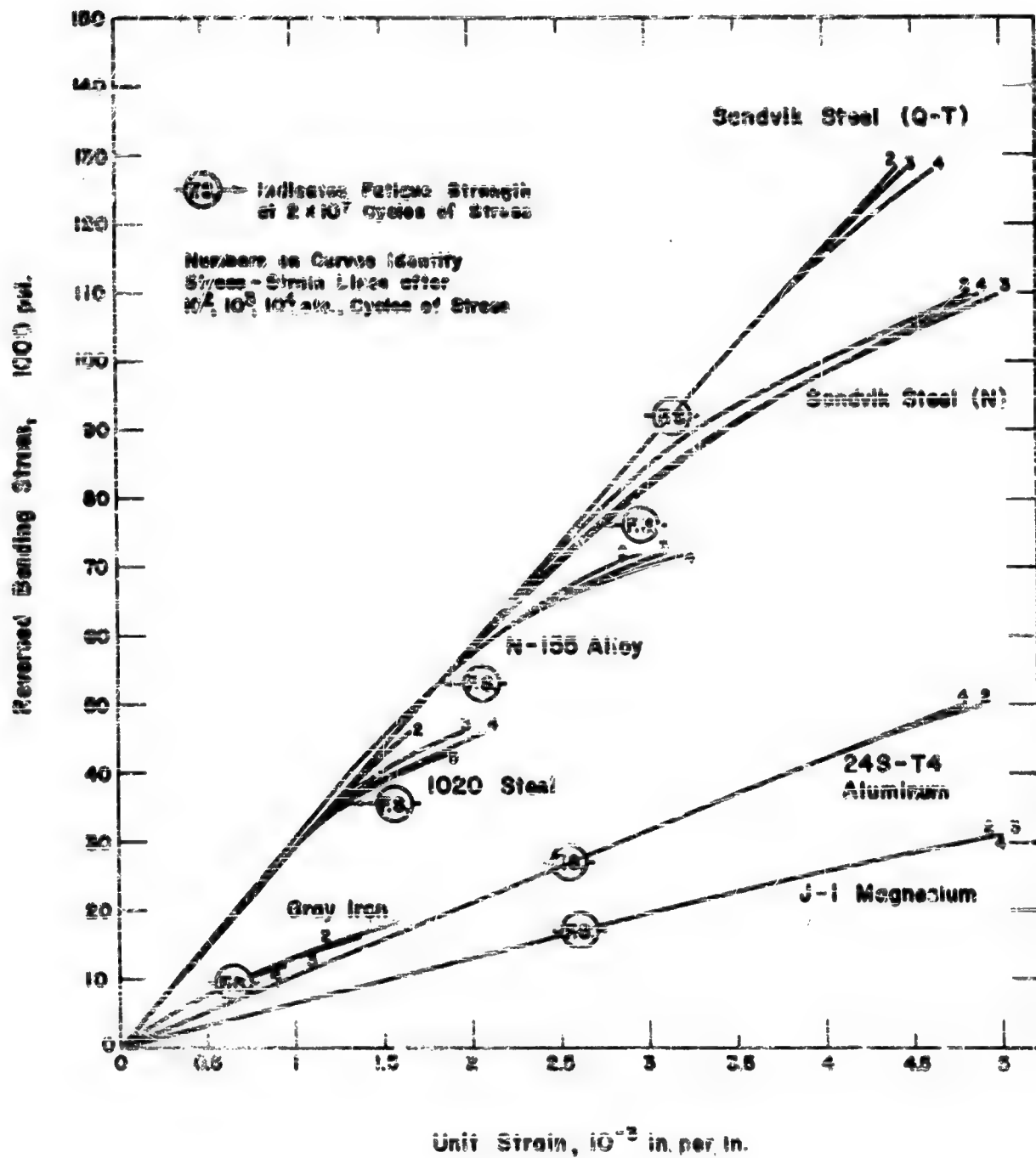
Fig. 7 — Dynamic Stress-Strain Curves in Bending for Unnotched Specimens of Various Materials at Room Temperature.

49

Fig. 8 — Average Dynamic Secant Modulus of Elasticity for Various Materials Shown Both as a Function of Stress Magnitude and the Ratio of Cyclic Stress to Fatigue Strength at 2x10⁷ Cycles.
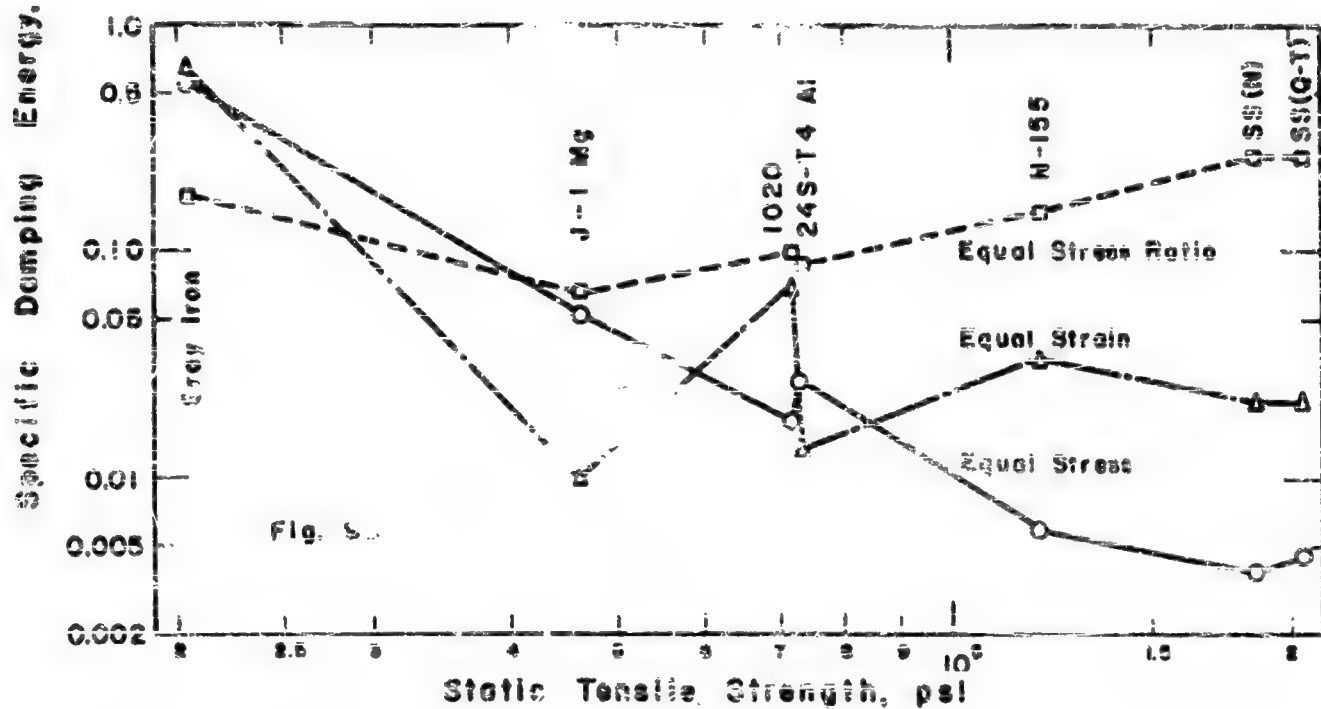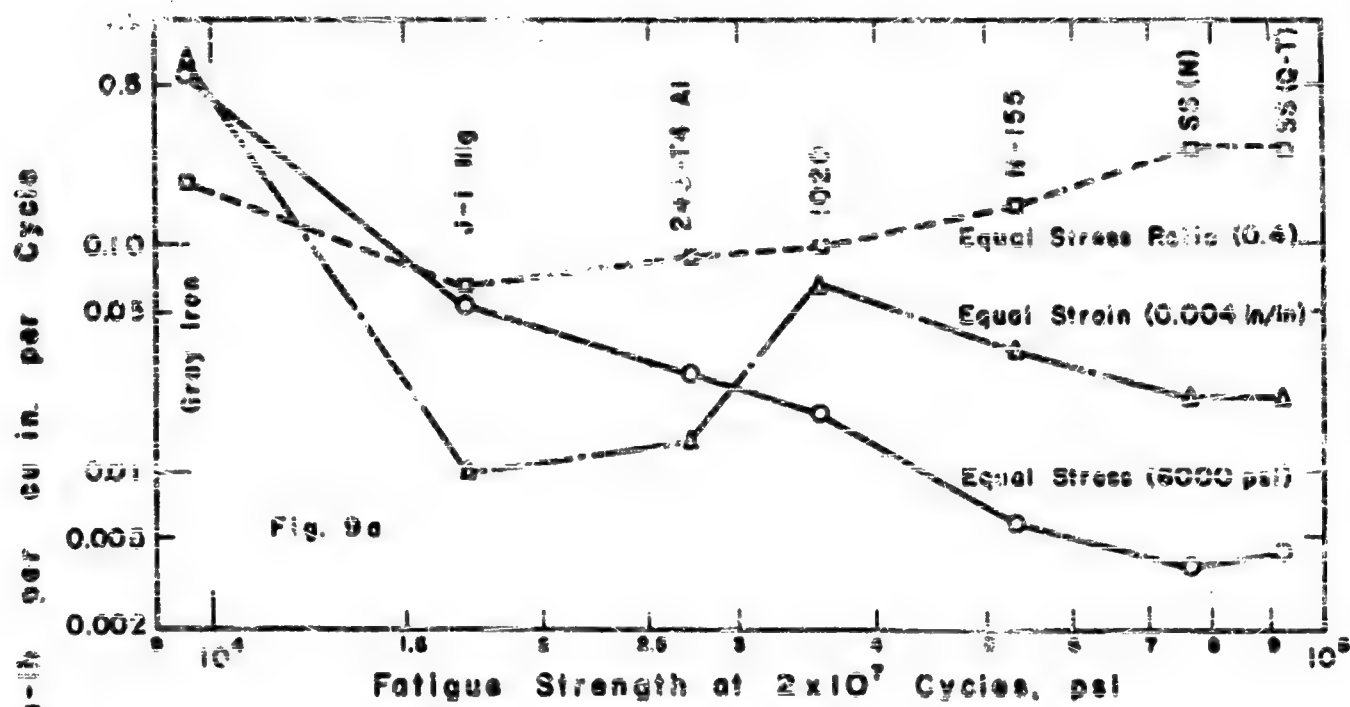
Fig. 9 — Specific Damping Energy on Three Different Bases of Comparison Shown Both as a Function of Fatigue Strength and Static Tensile Strength For Various Materials.
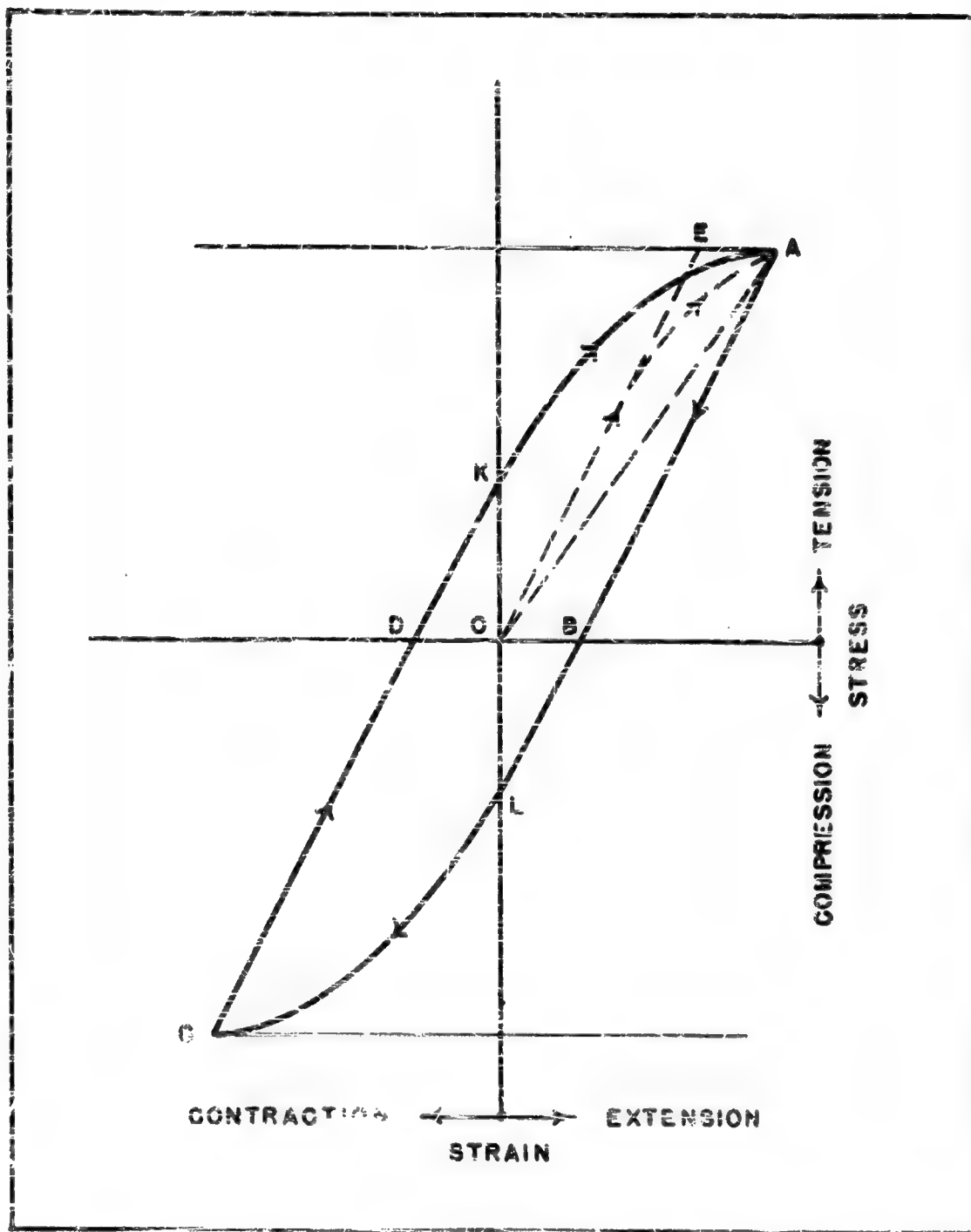
FIG. 10.—EXAGGERATED HYSTERESIS LOOP FOR A MATERIAL
SUBJECTED TO CYCLIC STRESS.
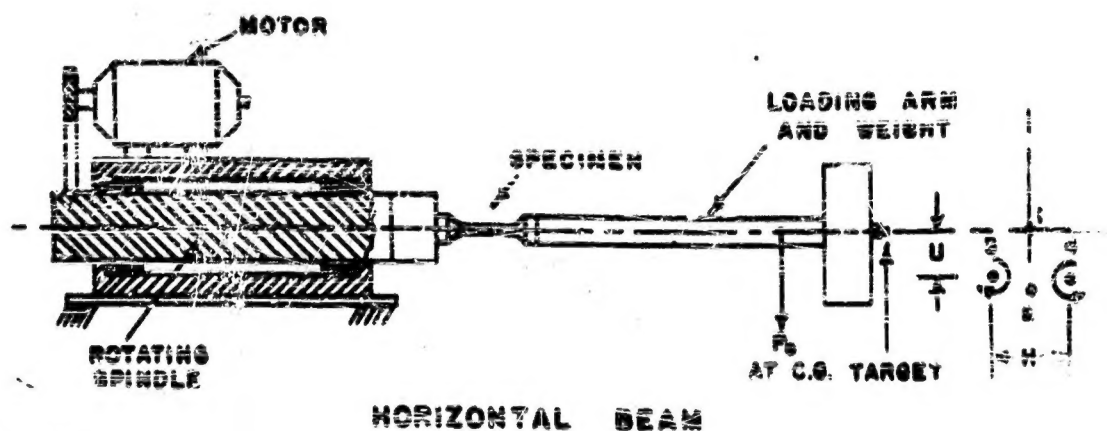
HORIZONTAL BEAM
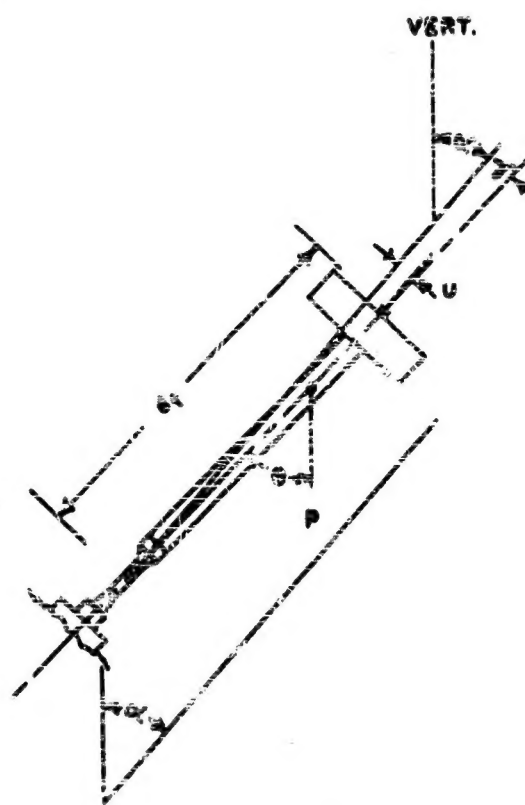
TILTING TABLE MACHINE

FIG. II.—HORIZONTAL AND VERTICAL DEFLECTION MEASUREMENTS IN ROTATING CANTILEVER BEAM DAMPING AND ELASTICITY TESTS.
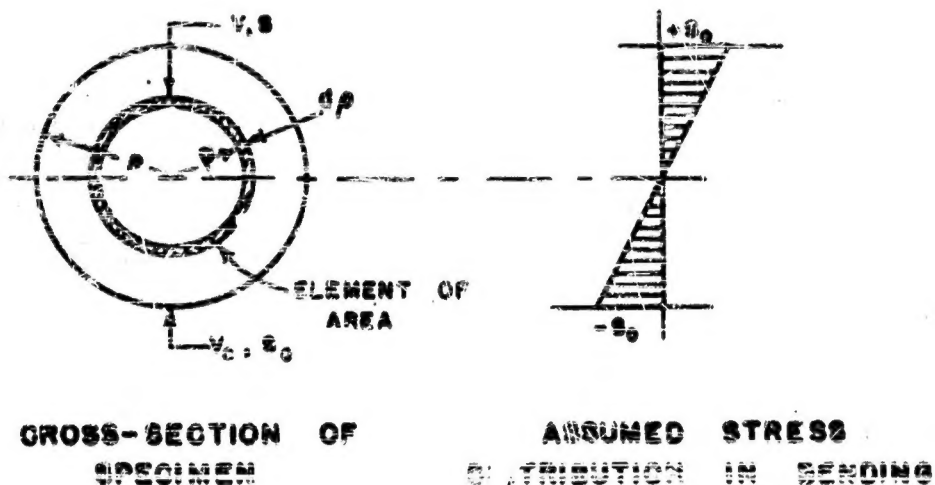
CROSS-SECTION OF
SPECIMEN

ASSUMED STRESS
DISTRIBUTION IN BENDING

FIG. 12 .—— DIAGRAM SHOWING CROSS-SECTION OF
ROTATING CANTILEVER SPECIMEN AND ASSUMED STRESS
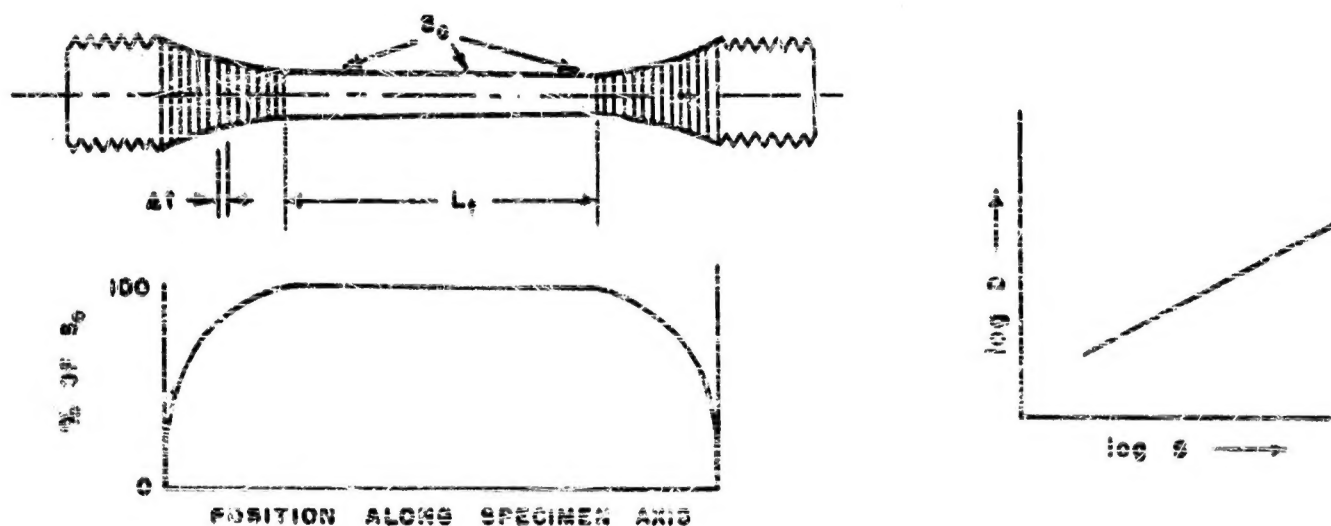DISTRIBUTION UNDER CONSTANT MAXIMUM BENDING STRESS.

FIG. 13 .—— SLICING OF SPECIMEN FILLETS FOR
APPROXIMATE INTEGRATION, VARIATION OF MAXIMUM STRESS
ALONG SPECIMEN AXIS, AND ASSUMED VARIATION OF
SPECIFIC DAMPING, D, WITH STRESS, S, IN THE DETERMINATION
OF GAGE-LENGTH EQUIVALENT OF SPECIMEN FILLETS.
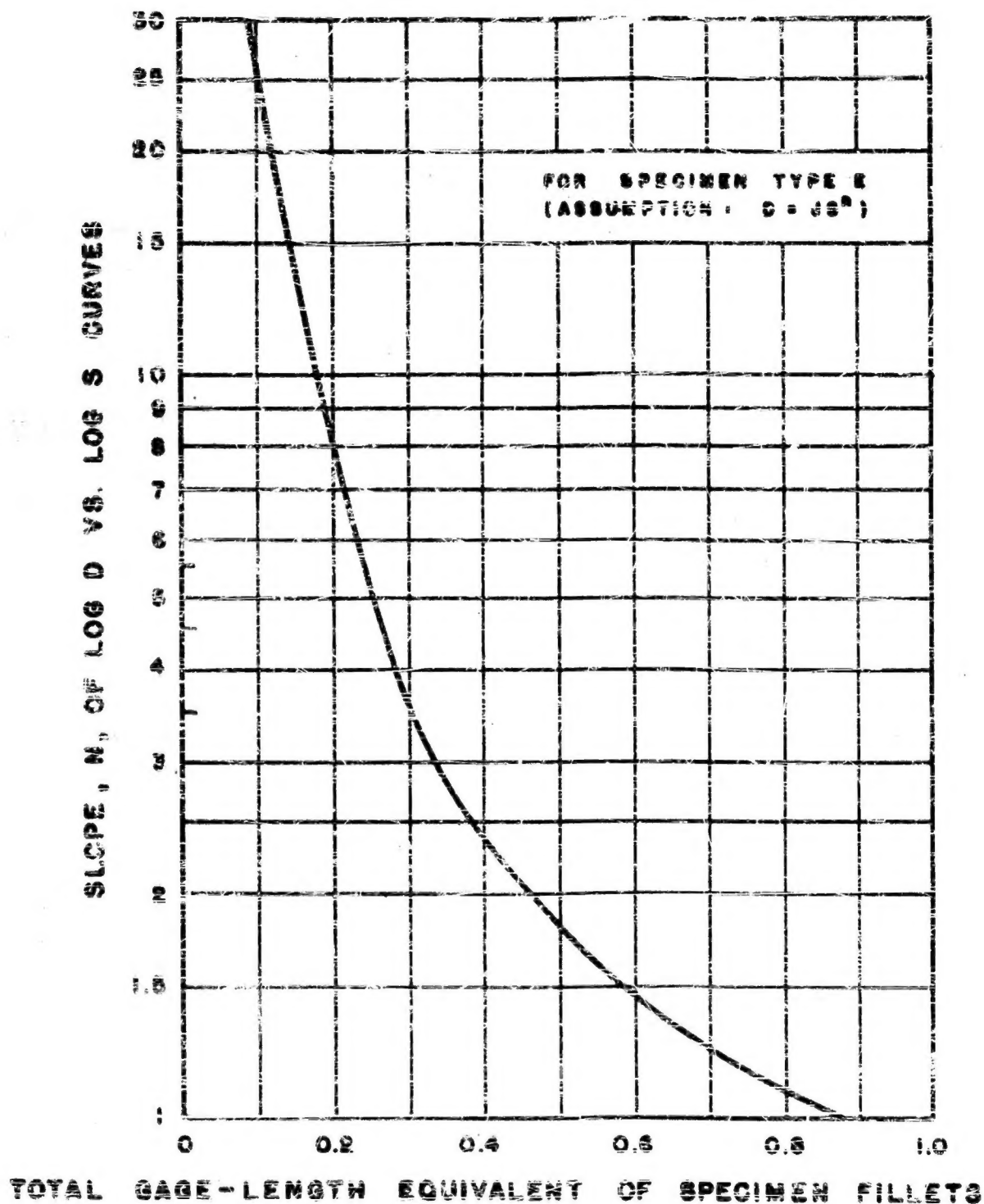
54

TOTAL GAGE-LENGTH EQUIVALENT OF SPECIMEN FILLETS

FIG. 14. — CURVE FOR DETERMINING TOTAL GAGE-LENGTH
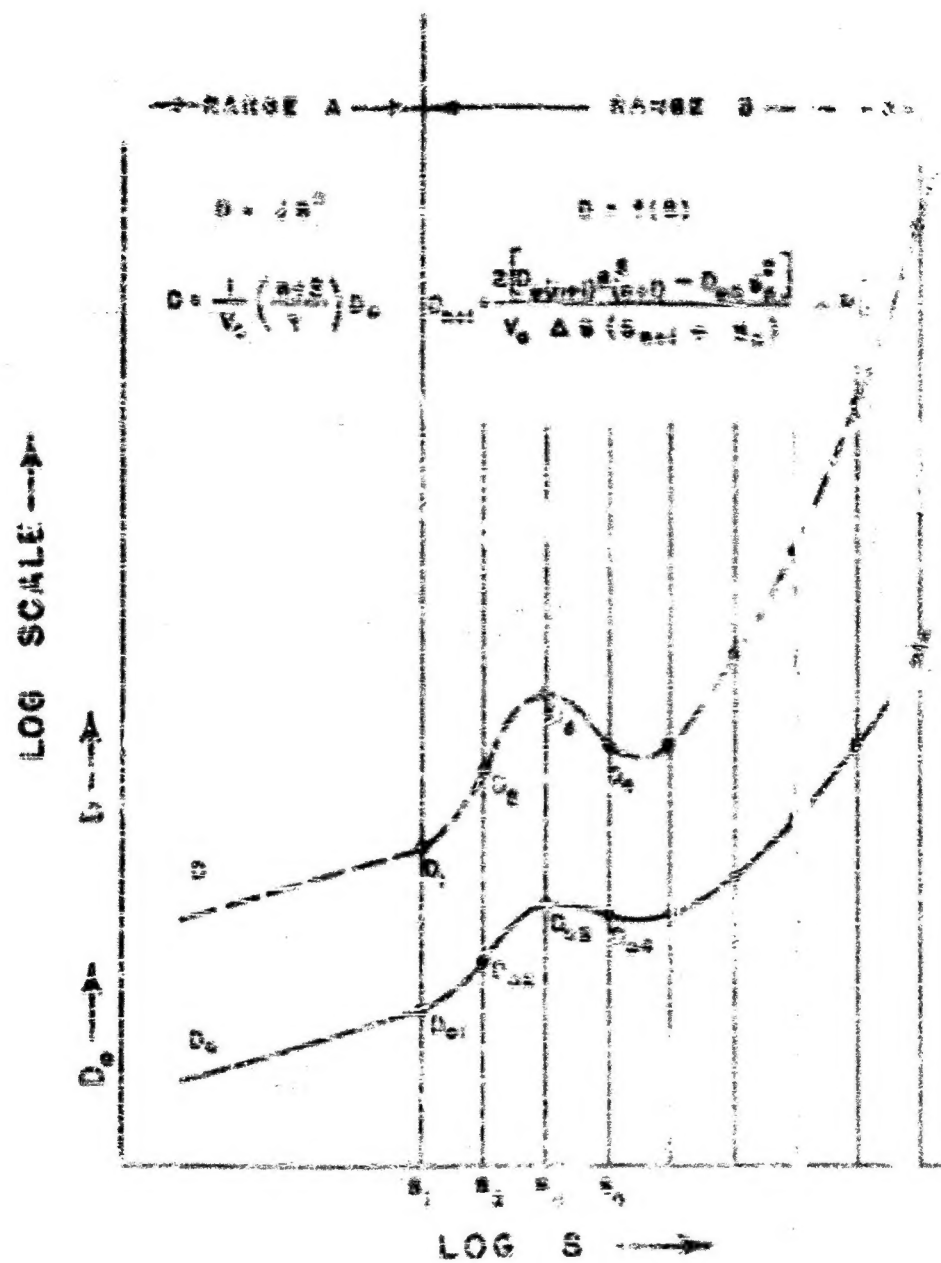EQUIVALENT OF FILLETS FOR ROTATING BENDING DAMPING
SPECIMEN TYPE E.

FIG. 15. — CONVERSION FROM TOTAL
DAMPING, D_o, TO SPECIFIC DAMPING, D.